Received: 17 July 2020 | Revised: 26 April 2021 | Accepted: 29 April 2021

DOI: 10.1111/bph.15532

RESEARCH PAPER

NLRP3 at the crossroads between immune/inflammatory responses and enteric neuroplastic remodelling in a mouse model of diet-induced obesity

Carolina Pellegrini[1,2] | Matteo Fornai[3] | Laura Benvenuti[3] | Rocchina Colucci[4] | Valentina Caputi[4,5] | Pablo Palazon-Riquelme[2] | Maria Cecilia Giron[4] | Anna Nericcio[4] | Francesca Garelli[4] | Vanessa D'Antongiovanni[3] | Cristina Segnani[3] | Chiara Ippolito[3] | Monica Nannipieri[3] | Gloria Lopez-Castejon[2] | Pablo Pelegrin[6] | György Haskó[7] | Nunzia Bernardini[3,8] | Corrado Blandizzi[3] | Luca Antonioli[3]

[1]Department of Pharmacy, University of Pisa, Pisa, Italy

[2]Lydia Becker Institute of Immunology and Inflammation, Division of Infection, Immunity and Respiratory Medicine, Faculty of Biology, Medicine and Health, University of Manchester, Manchester Academic Health Science Centre, Manchester, UK

[3]Department of Clinical and Experimental Medicine, University of Pisa, Pisa, Italy

[4]Department of Pharmaceutical and Pharmacological Sciences, University of Padova, Padua, Italy

[5]APC Microbiome Ireland, University College Cork, Cork, Ireland

[6]Biomedical Research Institute of Murcia (IMIB-Arrixaca), Hospital Clínico Universitario Virgen de la Arrixaca, Murcia, Spain

[7]Department of Anesthesiology, Columbia University, New York, New York, USA

[8]Interdepartmental Research Center "Nutraceuticals and Food for Health", University of Pisa, Pisa, Italy

Correspondence
Dr. Carolina Pellegrini, Department of Pharmacy, University of Pisa, via Bonanno, 6-56126 Pisa, Italy.
Email: carolina.pellegrini87@gmail.com

Background and Purpose: Enteric neurogenic/inflammation contributes to bowel dysmotility in obesity. We examined the role of NLRP3 in colonic neuromuscular dysfunctions in mice with high-fat diet (HFD)-induced obesity.

Experimental Approach: Wild-type C57BL/6J and NLRP3-KO (*Nlrp3*$^{-/-}$) mice were fed with HFD or standard diet for 8 weeks. The activation of inflammasome pathways in colonic tissues from obese mice was assessed. The role of NLRP3 in in vivo colonic transit and in vitro tachykininergic contractions and substance P distribution was evaluated. The effect of substance P on NLRP3 signalling was tested in cultured cells.

Key Results: HFD mice displayed increased body and epididymal fat weight, cholesterol levels, plasma resistin levels and plasma and colonic IL-1β levels, colonic inflammasome adaptor protein apoptosis-associated speck-like protein containing caspase-recruitment domain (ASC) and caspase-1 mRNA expression and ASC immunopositivity in macrophages. Colonic tachykininergic contractions were enhanced in HFD mice. HFD NLRP3$^{-/-}$ mice developed lower increase in body and epididymal fat weight, cholesterol levels, systemic and bowel inflammation. In HFD *Nlrp3*$^{-/-}$ mice, the functional alterations of tachykinergic pathways and faecal output were normalized. In THP-1 cells, substance P promoted IL-1β release. This effect was inhibited upon incubation with caspase-1 inhibitor or NK_1 antagonist and not observed in ASC$^{-/-}$ cells.

Abbreviations: ASC, apoptosis-associated speck-like protein containing a caspase-recruitment domain; HFD, high-fat diet; IL-1β, interleukin-1beta; L-NAME, N$^{\omega}$-nitro-L-arginine methylester; LPS, lipopolysaccharide; MyD88, adaptor molecule myeloid differentiation primary response 88; NLRP3, nucleotide-binding oligomerization domain leucine rich repeat and pyrin domain containing protein 3; SD, standard diet; WT, wild type.

Carolina Pellegrini and Matteo Fornai equally contributed to the manuscript.

Prof. Rocchina Colucci, Department of Pharmaceutical and Pharmacological Sciences, University of Padova, via largo Meneghetti, 2-35131, Padua, Italy.
Email: rok.colucci@gmail.com

Funding information
University of Pisa, Grant/Award Number: PRA_2020_46

Conclusion and Implications: In obesity, NLRP3 regulates an interplay between the shaping of enteric immune/inflammatory responses and the activation of substance P/NK_1 pathways underlying the onset of colonic dysmotility. Identifying NLRP3 as a therapeutic target for the treatment of bowel symptoms related to obesity.

KEYWORDS
colonic motility, high-fat diet, inflammation, macrophages, NLRP3 inflammasome, obesity, substance P, tachykinin neurotransmission

1 | INTRODUCTION

Growing evidence supports the view that obesity is characterized by a low-grade systemic inflammation, which could contribute to the onset of several chronic disorders, including type 2 diabetes mellitus, cardiovascular diseases, hepatic and kidney dysfunctions and cognitive impairment (Andersen et al., 2016; Rodriguez-Hernandez et al., 2013). Of note, obese patients can develop also digestive disorders, including constipation and infrequent bowel movements, which may impact negatively on patients' quality of life, thus complicating their clinical management (Gallagher et al., 2007). In particular, neuroplastic changes in the enteric nervous system, alterations of intestinal mucosal permeability and enteric inflammation have been proposed to be involved in the development of bowel motor dysfunctions associated with obesity (Lam et al., 2012; Raybould, 2012).

In a recent study, we observed that high-fat diet (HFD)-induced obesity is associated with an enhancement of enteric excitatory tachykinin neurotransmission along with colonic inflammation, indicating their possible contribution to bowel motor abnormalities (Antonioli et al., 2019). In addition, we showed that peritoneal macrophage depletion in obese mice counteracted enteric inflammation and the morpho-functional alterations of tachykinin pathways in the colonic neuromuscular compartment, suggesting that macrophages can contribute significantly to the colonic dysmotility associated with obesity, through an involvement of excitatory tachykinin pathways (Antonioli et al., 2019). However, the molecular mechanisms underlying the interplay between intestinal innate immune/inflammatory cells and enteric tachykinin pathways in the presence of obesity remain unclear.

In the setting of obesity, the **nucleotide-binding oligomerization domain leucine rich repeat and pyrin domain containing protein 3 (NLRP3)** inflammasome multiprotein complex has been found to act as a key immune sensor involved in the pathogenesis of immune/inflammatory responses, through the processing and release of **interleukin-1beta (IL-1β)** (Stienstra et al., 2011; Vandanmagsar et al., 2011). Indeed, clinical evidence has documented an overactivation of NLRP3 signalling, characterized by an increase in **caspase-1** activity and IL-1β levels, in peripheral blood monocytes from obese and type 2 diabetes mellitus patients, as compared with healthy subjects, thus supporting a critical role of the pro-inflammatory IL-1β cytokine in obesity-associated inflammation and type 2 diabetes mellitus (Donath et al., 2010; Lee et al., 2013). Of note, some studies have reported that NLRP3 can also play a protective role in liver inflammation associated with obesity (Pierantonelli et al., 2017). However, the beneficial effects resulting from in vivo pharmacological modulation of NLRP3 in animal models of metabolic and inflammatory disorders have led to assume that the inhibition of NLPR3 could represent a suitable pharmacological approach for the treatment of obesity and related comorbidities (Yang et al., 2016; Yang & Lim, 2014).

Based on the above background, the present research work was focused on investigating the involvement of NLRP3 inflammasome in the mechanisms underlying the development of bowel dysmotility associated with obesity, paying attention to its role in the interplay between immune/inflammatory responses and enteric substance P/NK_1 neuronal pathways. Our results provide new insights into a better understanding of the mechanisms underlying bowel motor dysfunctions associated with obesity, thus allowing to identify novel pharmacological targets for potential therapeutic interventions.

What is already known

- Obese patients experience digestive disorders, which impact negatively on their quality of life and clinical management.
- Enteric neuroplasticity, altered mucosal permeability and enteric inflammation contribute to bowel motor dysfunctions in obesity.

What does this study add

- NLRP3 acts as a regulatory hub linking enteric innate immune/inflammatory cells with substance P/NK_1 neuronal pathways.
- NLRP3 takes a relevant part in the pathophysiology of enteric motor disorders associated with obesity.

What is the clinical significance

- NLRP3 may represent a potential therapeutic target for the treatment of bowel dysfunctions in obesity.

2 | METHODS

2.1 | Animal model of diet-induced obesity

Six-week-old male C57BL/6 wild type (WT) (RRID:MGI:5658455, Envigo, Udine, Italy) and C57BL/6 *Nlrp3* KO ($^{-/-}$) (RRID: IMSR_JAX:021302) animals (kindly donated by Prof Pablo Pelegrin (Biomedical Research Institute of Murcia, Murcia, Spain) (20- to 25-g body weight) were employed throughout the study. Mice were fed with HFD (60% calories from fat, TD.06414) or standard diet (SD, 18% calories from fat; TD.2018) for 8 weeks (eight mice per each group). HFD provided 18.3% kcal as proteins, 21.4% kcal as carbohydrates and 60.8% kcal as fat (5.1 kcal·g^{-1}), whereas SD provided 24% kcal as proteins, 58% kcal as carbohydrates and 18% kcal as fat (3.1 kcal·g^{-1}).

HFD and SD were purchased from ENVIGO. The animals were housed, three in a cage, in temperature-controlled rooms on a 12-h light cycle at 22–24°C and 50%–60% humidity, with water and food availability ad libitum. After 8 weeks of SD or HDF, animals were killed by asphyxiation with CO_2. Of note, after 8 weeks of HFD, mice are characterized by increase in body and epidydimal fat weight and cholesterol, glucose and triglycerides levels, while no signs of insulin resistance are detected. These metabolic alterations represent conditions strikingly reflecting those observed in obese patients not yet diabetic (Antonioli et al., 2019; Csoka et al., 2017; Raybould, 2012).

All the procedures involving animals were carried out following the guidelines of the European Community Council Directive 86-609 and in accordance with the Code of Ethics of the World Medical Association (Declaration of Helsinki, EU Directive 2010/63/EU for animal experiments). The experiments were approved by the Ethical Committee of the University of Pisa (Protocol number 0037321/2013) and by the Italian Ministry of Health (authorization number 674/2016-PR). All efforts to reduce and minimize the number of animals, and their suffering were carried out. Animal studies are reported in compliance with the ARRIVE guidelines (Percie du Sert et al., 2020) and with the recommendations made by the *British Journal of Pharmacology* (Lilley et al., 2020). A randomization of animals between groups was carried out in order to generate groups of equal size. The investigators responsible for data analysis were blind to which animals represent WT SD and HFD mice as well as SD and HFD *Nlrp3*$^{-/-}$ animals. The design in this study complies with the recommendations on experimental design in pharmacology (Curtis et al., 2018).

2.2 | Measurement of body weight, epididymal fat weight and food and energy intake

Body weight was measured once a week throughout the 8 weeks of HFD or SD. Energy intake was measured daily for 8 weeks on the basis of the caloric content of HFD (5.1 kcal·g^{-1}) or SD (3.1 kcal·g^{-1}). Food intake was measured and changed daily. Food intake was calculated by weighing all remnants of pellets at 11:00, including any spilled food in cages and subtracting this value from the initial weight. During these measurements, all mice were housed individually. At the time of experiment, the epididymal fat was quickly dissected out and weighed.

2.3 | Measurement of cholesterol levels

Blood samples were taken from the tail after overnight starvation and cholesterol levels were measured using multiCare-in sensor (BSI Srl, Arezzo, Italy), in accordance with the manufacturer's instructions.

2.4 | Evaluation of plasma resistin levels in mice

Plasma resistin levels were measured by an enzyme-linked immunosorbent assay (ELISA) kit (Abcam ab205574, detection limits 31.25–2000 pg·ml^{-1}). For this purpose, 0.5 ml of fasting venous blood was collected in K2-coated tubes containing 30 μl (0.5 mol·L^{-1}) of EDTA plus 2000 KIU of aprotinin. Samples were mixed and centrifuged at 2000 g for 20 min. After centrifugation, 2 ml of cold acetone (4°C) was added to 0.5 ml of plasma, mixed and centrifuged at 2000 g for 20 min at 4°C. The supernatant was added to 4 ml of cold petroleum ether, mixed, centrifuged and dried under a vacuum to remove any residual acetone. Samples were then stored at −20°C until use. Aliquots of plasma were diluted 1:50 and used for the assay. Plasma resistin levels were expressed as nanograms per millilitre.

2.5 | Evaluation of plasma and tissue IL-1β levels in mice

Plasma IL-1β levels were measured by an enzyme-linked immunosorbent assay (ELISA) kit (R&D systems, detection limits 3.9–2000 pg·ml^{-1}), as described previously (Antonioli, Moriconi, et al., 2020). The Merck Millipore Amicon™ Ultra Centrifugal Filter Units was used to concentrate samples.

For this purpose, 0.5 ml of fasting venous blood was collected in K2-coated tubes containing 30 μl (0.5 mol·L^{-1}) of EDTA plus 2000 KIU of aprotinin. Samples were mixed and centrifuged at 2000 g for 20 min. After centrifugation, 2 ml of cold acetone (4°C) was added to 0.5 ml of plasma, mixed and centrifuged at 2000 g for 20 min at 4°C. The supernatant was added to 4 ml of cold petroleum ether, mixed, centrifuged and dried under a vacuum to remove any residual acetone. Samples were then stored at −20°C until use. Plasma IL-1β levels were expressed as picograms per millilitre.

IL-1β levels in colonic tissues were measured by an ELISA kit (R&D system, detection limits 3.9–2000 pg ml^{-1}), as described previously (Pellegrini et al., 2016). For this purpose, colonic tissue samples, stored previously at −80°C, were weighed, thawed and homogenized in 0.4-ml PBS, pH 7.2/20 mg of tissue at 4°C, and centrifuged at 10,000 g for 5 min. Aliquots (100 μl) of supernatants were then used for the assay. Tissue IL-1β levels were expressed as picograms per milligram of tissue.

2.6 | RNA extraction and quantitative real-time PCR for ASC and caspase-1

Total RNA was isolated from colonic tissues (20 mg) using TRIzol reagent (Invitrogen, Life Technologies, Thermo Fisher Scientific Inc., CA, USA) according to the manufacturer's instructions. The concentration of isolated RNA was determined with a spectrophotometer, and two micrograms of RNA were used for the reverse transcription (RT) procedure (High Capacity cDNA Reverse Transcription Kit, Applied Biosystems, Thermo Fisher Scientific Inc., CA, USA). RT was performed in a mixture of 2-µl RT buffer, 0.8-µl dNTP, 2-µl random primer, 1-µl reverse transcriptase and nuclease-free water (Amresco LLC, Solon, USA) up to 10 µl. PCR cycles (Veriti 96-Well Thermal Cycler, Applied Biosystems, Thermo Fisher Scientific Inc., CA, USA) were set as follows: 25°C for 10 min, 37°C for 120 min and 85°C for 5 min. Ten-fold dilution of cDNA was used for RT-qPCR procedure. Specific primers for GAPDH (*Gapdh*, QT01658692) were purchased from Qiagen (QuantiTech Primer Assays). Primers for ASC (*Pycard*) and caspase-1 (*Casp1*) were designed using the primer express 3.0.1 software and obtained from Sigma. Primer sequences are as follows: mCasp1-Fw: CGTACACGTCTTGCCCTCATTA; mCasp1-Rv; CCAA CCCTCGGAGAAAGATG; mASC-Fw: TCATTGCCAGGGTCACAGAA; mASC-Rv: CACACTGCCATGCAAAGCA; qPCR was performed using Power SYBR® Green PCR mastermix (Applied Biosystems, 4385618) and Quantistudio 12K Flex (Applied Biosystems). Melting curves from this qPCR are showed in Figure S1a–c. Gene expression was calculated using the ΔΔCt method. Data were normalized to expression levels of the housekeeping gene GAPDH across each treatment and fold change was expressed relative to basal RNA levels from control animals. No difference in colonic GAPDH expression was detected between SD and HFD mice (Figure S2).

Primers specificity is also shown in Figure S1. This primer specificity validation was performed in cDNA samples obtained from Bone Marrow Derived Macrophages treated with LPS (1 µg·ml^{-1}; 4 h) as in Lopez-Castejon et al. (2013). RNA and cDNA were generated as above. Specificity of the primers was confirmed by (i) presence of just one amplicon visualized by running the caspase-1, ASC and GAPDH qPCR products in a 2% DNA agarose gel (Figure S1d) and (ii) qPCR amplicon sequencing coinciding with its corresponding predicted sequence (Figure S1e–h). PCR product was purified using Illustra ExoProStar kit (Cytiva, US78210) following manufacturer instructions) and sequenced by Sanger sequencing at the Genomic and Technologies Facility at the University of Manchester (UK).

2.7 | Evaluation of tissue caspase-1 expression in mice

The Immuno-related procedures used comply with the recommendations made by the *British Journal of Pharmacology* (Alexander et al., 2018). Colonic tissues were weighed and homogenized in lysis buffer, using a polytron homogenizer, as described by Fazzini et al. (2014) and Richter et al. (2018). Proteins were quantified with the Bradford assay. Proteins were separated onto a pre-cast 4%–20% polyacrylamide gel (Mini-PROTEAN TGX gel, Biorad) and transferred to PVDF membranes (Trans-Blot TurboTM PVDF Transfer packs, Biorad). Membranes were blocked with 3% BSA diluted in tris-buffered saline (TBS, 20-mM Tris-HCl, PH 7.5, 150-mM NaCl) with 0.1% Tween 20. Primary antibodies against β-actin (monoclonal; 1:5000) and caspase-1 (polyclonal; 1:1000) were used. Appropriate secondary anti-mouse and anti-rabbit IgG antibodies were used). Protein bands were detected with ECL reagents (Clarity™ Western ECL Blotting Substrate, Biorad). Densitometry was performed by ImageJ software.

2.8 | Confocal immunofluorescence histochemistry

Sections (7 µm) from formalin-fixed/paraffin-embedded colonic and spleen samples were processed for F4/80-ASC double immunofluorescence. F4/80 was used as mouse macrophage surface marker, and ASC as marker of inflammasome activation in macrophages (Antonioli et al., 2019; Hume et al., 1984; Lopez-Castejon et al., 2013; Pelegrin & Surprenant, 2009; Shi et al., 2012; Tejera et al., 2019). After heat unmasking and blocking non-specific binding, sections were incubated overnight with the following combined primary antibodies: rat anti-F4/80 (1:10) and rabbit anti-ASC (1:25). They were then treated with appropriate fluorophore-conjugated secondary antibody or biotinylated secondary antibody plus fluorophore-conjugated streptavidin and, finally, stained with nuclear TO-PRO3 as previously described (Ippolito et al., 2016). Immunofluorescent stainings were examined under a Leica TCS SP8 confocal laser-scanning microscope (Leica Microsystems, Mannheim, Germany). The antibody specificity was tested on spleen (red pulp) from HDF mouse being a good positive control organ for both F4/80 (Lin et al., 2005) and ASC (Masumoto et al., 2001). In addition, the supplemtation with HFD to mice is associated with the occurrence of immune/inflammatory responses characterized by inflammasome activation signalling in several tissues including the spleen (Souza et al., 2019). Negative controls for each set of tissues were obtained by omitting the primary antibodies. The results obtained from these analyses were not subjected to statistical analyses because our intent was to confirm the activation of inflammasome complex in intestinal immune/inflammatory cells in the colonic *lamina propria*, from HFD mice.

2.9 | Evaluation of faecal output

Faecal output was recorded from 8:00 AM to 9:00 AM on each day. Each animal was removed from its cage and placed in a clean plastic cage without food and water for 1 h. Stools were collected immediately after expulsion, placed in sealed tubes and counted. In this context, though putting animals in a clean cage for 1 h can represent a repeated model of environmental mild stress (Casadesus et al., 2001; Fuchs et al., 2013; Kataoka et al., 2020; Morimoto et al., 1993), WT and KO SD and HFD animals displayed no changes in food intake,

regarded as behavioural alteration related to stress (Bremner et al., 2000).

2.10 | Recording of contractile activity

The contractile activity of colonic longitudinal smooth muscle was recorded as described previously (Antonioli et al., 2011, 2017; D'Antongiovanni, Benvenuti, et al., 2020). After killing, the colon was removed and placed in cold Krebs solution. Longitudinal and circular muscle strips from distal colon, approximately 4 mm wide and 10 mm long, were set up in organ baths containing Krebs solution at 37°C, bubbled with 95% O_2 + 5% CO_2. The strips were connected to isometric force transducers (2Biological Instruments, Besozzo, VA, Italy). A tension of 0.5 g was slowly applied to each preparation. Mechanical activity was recorded by BIOPAC MP150 (2Biological Instruments). Krebs solution had the following composition (in millimolar): NaCl 113, KCl 4.7, $CaCl_2$ 2.5, KH_2PO_4 1.2, $MgSO_4$ 1.2, $NaHCO_3$ 25 and glucose 11.5 (pH 7.4 ± 0.1). Each preparation was allowed to equilibrate for at least 30 min, with intervening washings at 10-min intervals. A pair of coaxial platinum electrodes was positioned at a distance of 10 mm from the longitudinal axis of each preparation to deliver transmural electrical stimulation by a BM-ST6 stimulator (Biomedica M+ 07angoni, Pisa, Italy). Electrical stimuli were applied as follows: 10-s single trains (ES) consisting of square wave pulses (0.5 ms, 30 mA). At the end of the equilibration period, each preparation was repeatedly challenged with electrical stimuli (10 Hz), and experiments were started when reproducible responses were obtained (usually after two or three stimulations).

Preliminary experiments were performed to select the frequency of electrical stimulation and the exogenous substance P concentration eliciting submaximal contractions, suitable to better appreciate changes in the colonic contractile responses. For this purpose, colonic preparations, obtained from either SD or HFD animals, were challenged with single trains of electrical stimuli (ES) at increasing frequencies, ranging from 1 to 20 Hz. Frequency–response curves were constructed under the following in vitro experimental conditions adopted in the present study:- (1) standard Krebs solution, (2) Krebs solution added with **N^{ω}-nitro- L-arginine methylester (L-NAME**; 100 μM), **guanethidine** (10 μM), **5-fluoro-3-[2-[4-methoxy-4-[[(R)-phenylsulphinyl]methyl]-1-piperidinyl]ethyl]-1H-indole (GR159897**, NK_2 receptor antagonist; 1 μM), **(R)-[[(2-phenyl-4-quinolinyl) carbonyl]amino]-methyl ester benzeneacetic acid (SB 218795**, NK_3 receptor antagonist; 1 μM) and **atropine** (1 μM). Concentration–response curves to exogenous substance P were constructed at concentrations ranging from 0.01 to 100 μM in the presence of **tetrodotoxin** (1 μM). These preliminary experiments allowed to select the frequency of 10 Hz and the concentration of 10 μM of exogenous substance P, eliciting submaximal contractions suitable for investigating the changes in colonic contractions. The tension developed by each preparation (grams) was normalized by the wet tissue weight (g/g tissue).

In the first set of experiments, contractions were recorded from colonic preparations maintained in Krebs solution containing L-NAME (100 μM), guanethidine (10 μM), GR159897 (1 μM), SB 218795 (1 μM) and atropine (1 μM) to examine the patterns of colonic contractions driven by excitatory nerve NK_1 receptor mediated pathways.

In the second series, colonic contractions were evoked by direct pharmacological activation of NK_1 receptors located on smooth muscle cells. For this purpose, colonic preparations were maintained in Krebs solution containing tetrodotoxin (1 μM) and stimulated with exogenous substance P (10 μM).

2.11 | In vitro assays on NLRP3 inflammasome

WT and ASC knock out ($ASC^{-/-}$) human monocytic cell lines (THP-1) were kindly donated by Prof Veit Hornung (Ludwig Maximilian, University of Munich) and cultured in RPMI 1640 media (Sigma) supplemented with 10% FBS (PAA Laboratories), 100 units per millilitre penicillin and 100 $\mu g \cdot ml^{-1}$ streptomycin (Sigma) (Schmid-Burgk et al., 2015).

Cells were plated in 24-well plates at a density of 5×10^5 cells per well and treated with phorbol 12-myristate 13-acetate (PMA, 0.5 μM for 3 h), regarded as a standard in vitro method to differentiate THP-1 cells in a macrophage-like cells (Lopez-Castejon et al., 2013; Palazon-Riquelme et al., 2018).

After 3 h, the medium was removed, fresh media was added and cells were incubated overnight (37°C, 5% CO_2).

In the first series of experiments, cells were LPS-primed (1 $\mu g \cdot ml^{-1}$ for 4 h) as previously described by Palazon-Riquelme et al. (2018). In particular, the dose and timing of LPS is known to induce innate immune signalling, including **toll-like receptor** (TLR)-adaptor molecule myeloid differentiation primary response88 (MyD88), that promote pro-IL-1 and NLRP3 transcription through **nuclear factor-κB (NF-κB)** activation (first step of NLRP3 inflammasome activation) (Pellegrini et al., 2017). In addition, **LPS** priming mimics the in vivo inflammation associated with HFD exposure (Kim et al., 2012). After 4 h, LPS-primed cells were treated with nigericin (standard NLRP3 inflammasome activator, 10 μM, 1 h) or substance P (10 μM, 2 h) as described by Lopez-Castejon et al. (2013).

In the second series of experiments, LPS-primed (1 $\mu g \cdot ml^{-1}$, 4 h) cells were treated for 15 min with vehicle (0.5% DMSO) or caspase-1 inhibitor (YVAD, 100 μM) before the addition of nigericin (10 μM, 1 h) or substance P (10 μM, 2 h) as described by Lopez-Castejon et al. (2013).

In the third series of experiments, LPS-primed (1 $\mu g \cdot ml^{-1}$, 4 h) $ASC^{-/-}$ THP-1 cells were treated with nigericin (10 μM, 1 h) or substance P (10 μM, 2 h).

In the fourth series of experiments, LPS-primed (1 $\mu g \cdot ml^{-1}$, 4 h) cells were treated for 30 min with vehicle (0.5% DMSO) or **L-732,138** (NK_1 receptor antagonist, 20 μM) before the addition of substance P (10 μM, 2 h) (Lai et al., 2006).

In the fifth series of experiments, LPS-primed (1 μg·ml^{-1}, 4 h) cells were treated for 30 min with vehicle (0.5% DMSO) or L-732,138 (NK_1 receptor antagonist, 1 μM) before the addition of substance P (10 μM, 2 h).

In the sixth series of experiments, LPS-primed (1 μg·ml^{-1}, 4 h) cells were treated for 30 min with vehicle (0.5% DMSO), GR159897 (NK_2 receptor antagonist, 1 μM) and SB 218795 (NK_3 receptor antagonist, 1 μM) before the addition of substance P (10 μM, 2 h).

In the seventh series of experiments, LPS-primed (1 μg·ml^{-1}, 4 h) cells were also treated for 30 min with vehicle (0.5% DMSO), GR159897 (NK_2 receptor antagonist, 1 μM) and SB 218795 (NK_3 receptor antagonist, 1 μM) and L-732,138 (NK_1 receptor antagonist, 1 μM) before the addition of substance P (10 μM, 2 h).

In the eighth series of experiments, LPS-primed (1 μg·ml^{-1}, 4 h) cells were treated for 2 h with vehicle (0.5% DMSO) or GR73632 (NK_1 receptor agonist 1 μM, 2 h).

WT and ASC$^{-/-}$ THP-1 treated with nigericin or substance P, in the presence or in the absence of YVAD or L-732,138, were incubated for 5 and 6 h, respectively, before the collection of supernatants and cell lysates for the analysis of IL-1β release.

Concentrations of substance P were selected on the basis of a previous study performed in phorbol 12-myristate 13-acetate-differentiated THP-1 cells (Cunin et al., 2011; Maslanik et al., 2013; Vallejo et al., 2014) and by preliminary experiments designed to assay increasing concentrations of substance P (1, 10 and 100 μM) on IL-1β levels in LPS-primed THP-1 cells.

Concentrations of GR73632were selected on the basis of a previous study performed in cell cultures and in vitro functional studies (Maslanik et al., 2013; Vallejo et al., 2014) and by preliminary experiments designed to assay increasing concentrations of substance P (0.1, 1 and 10 μM) on IL-1β levels in LPS-primed THP-1 cells.

Concentrations of GR159897 (NK_2 receptor antagonist, 1 μM) or SB 218795 (NK_3 receptor antagonist, 1 μM) were selected on the basis of a previous study performed in cell cultures (Maslanik et al., 2013; Vallejo et al., 2014).

2.11.1 | Cell death assay

Cell death was measured by quantitative assessment of lactate dehydrogenase (LDH) levels in the medium. CytoTox 96® Non-Radioactive Cytotoxicity Assay (Promega, G1780) was used in accordance with manufacturer instructions. Plates were read at 490 nm and results shown as percentage of LDH release relative to the total cells lysed.

2.11.2 | IL-1β release assay

IL-1β concentration in cell supernatants (dilution 1:5) was assessed by ELISA kit (R&D Systems, kit detection limits 3.91–250 pg·ml^{-1}), following the protocols provided by the manufacturer. IL-1β concentration was expressed as picograms per millilitre.

2.11.3 | ASC speck detection and quantification

Cells were plated as described above on glass coverslips. THP-1 cells were LPS-primed (1 μg·ml^{-1}, 4 h) and treated with nigericin (10 μM, 1 h) or LPS (1 μg·ml^{-1}, 6 h) and substance P (10 μM, 6 h). The cells were then fixed with 4% paraformaldehyde and 4% sucrose in PBS for 30 min. Afterwards, cells were permeabilized with 0.1% Triton X-100 and then quenched with 0.25% ammonium chloride. A blocking step for 1 h, by 5% BSA and 5% donkey serum (block solution), was used before incubation with rabbit anti-ASC (1:500) in blocking solution for 1 h. Coverslips were then washed in PBS. ASC antibodies were detected by incubation with Alexa Fluor 594 conjugated donkey anti-rabbit IgG antibody (1:1000) in blocking solution for 1 h. The coverslips were washed again with PBS and finally in distilled water before being dried and mounted onto a glass slide using ProLong Gold mounting medium containing DAPI (Invitrogen). Images were taken with an Olympus BX51 upright microscope using a 20 X/0.50 Plan Fln objective and captured using a Coolsnap EZ camera (Photometrics) through MetaVue Software (Molecular Devices). To quantify the extent of speck formation, the percentage of cells that contained an ASC speck was counted. Cells from 10 different fields (average of 200 cells/field for peritoneal macrophages and 650 cells/field for THP-1) were counted for each of the different experiments ($n = 6$). Images were analysed using ImageJ (rsb.info.nih.gov). The data are expressed as the percentage of ASC specks per number of cells per field.

2.12 | Data and statistical analysis

The data and statistical analysis comply with the recommendations of the *British Journal of Pharmacology* on experimental design and analysis in pharmacology (Curtis et al., 2018). The statistical analysis was undertaken only for studies where each group size was at least $n = 5$. In particular, the results are presented as mean ± standard error of the mean (SEM) of at least six independent experiments. All the group sizes were designed to be homogeneous. *n* refers to the number of mice or the number of individual experiments in cell cultures, and statistical analysis was carried out using these independent values. Outliers were defined as values that exceed the distance from the median value by 50%.

Data normalization was carried out for each evaluated parameter as described in each relative methods subsections. The analysis of the Gaussian distribution was carried out using Shapiro–Wilk normality test. The significance of differences was evaluated by Kruskal–Wallis test, one-way or two-way ANOVA followed by the appropriate post hoc test. Post hoc tests were conducted only if *F* in ANOVA (or equivalent) achieved a statistical significance lower than 0.05 and there was no significant variance inhomogeneity.

P values <0.05 were considered representative of significant statistical differences. All statistical procedures were performed by commercial software (GraphPad Prism, version 7.0, RRID: SCR_002798, GraphPad Software Inc., San Diego, CA, USA).

2.13 | Materials

Atropine sulphate, **substance P**, **guanethidine monosulphate**, nigericin, Ac-YVAD-cmk (**caspase-1** inhibitor), **bacterial lipopolysaccharide** (LPS, *Escherichia coli* O26:B6), dimethyl sulphoxide (DMSO), protease inhibitors, 1,10-Phenanthroline and N-Ethylmaleimide were purchased from Sigma Chemicals Co. (St. Louis, MO, USA). FBS was obtained from PAA Laboratories. **Tetrodotoxin**, 5-fluoro-3-[2-[4-methoxy-4-[[(R)-phenylsulphinyl]methyl]-1-piperidinyl] ethyl]-1H-indole, **GR159897**, **NK_2 receptor** antagonist), (R)-[[2-phenyl-4-quinolinyl)carbonyl]amino]-methyl ester benzeneacetic acid (SB 218795, **NK_3 receptor** antagonist), *N*-Acetyl-L-tryptophan 3,5-*bis* (trifluoromethyl)benzyl ester (**L-732,138**, **NK_1 receptor** antagonist), GR73632 (NK_1 receptor agonist), **N^{ω}-nitro-L-arginine methylester** (L-NAME) were obtained from Tocris (Bristol, UK). Neutral buffered formaldehyde and xylene were purchased from Carlo Erba, Milan, Italy. Nickel-intensified 3,3′-diaminobenzidine tetra-hydrochloride (DAB Substrate Kit for Peroxidase, Vector Laboratories Burlingame, CA, USA). The primary and secondary antibodies used for the Western blot were β-actin (monoclonal; 1:5000; Sigma Aldrich; A5316, RRID:AB_476743) and caspase-1 (polyclonal; 1:1000; Abcam; ab1872, RRID:AB_302644) and anti-mouse IgG (Abcam, ab97040, RRID:AB_10698223) and anti-rabbit IgG (Abcam, ab6721, RRID: AB_955447) antibodies, respectively. The primary antibodies used in Figure 3 for immunofluorescence analysis were rabbit anti-adaptor protein apoptosis-associated speck-like protein containing a

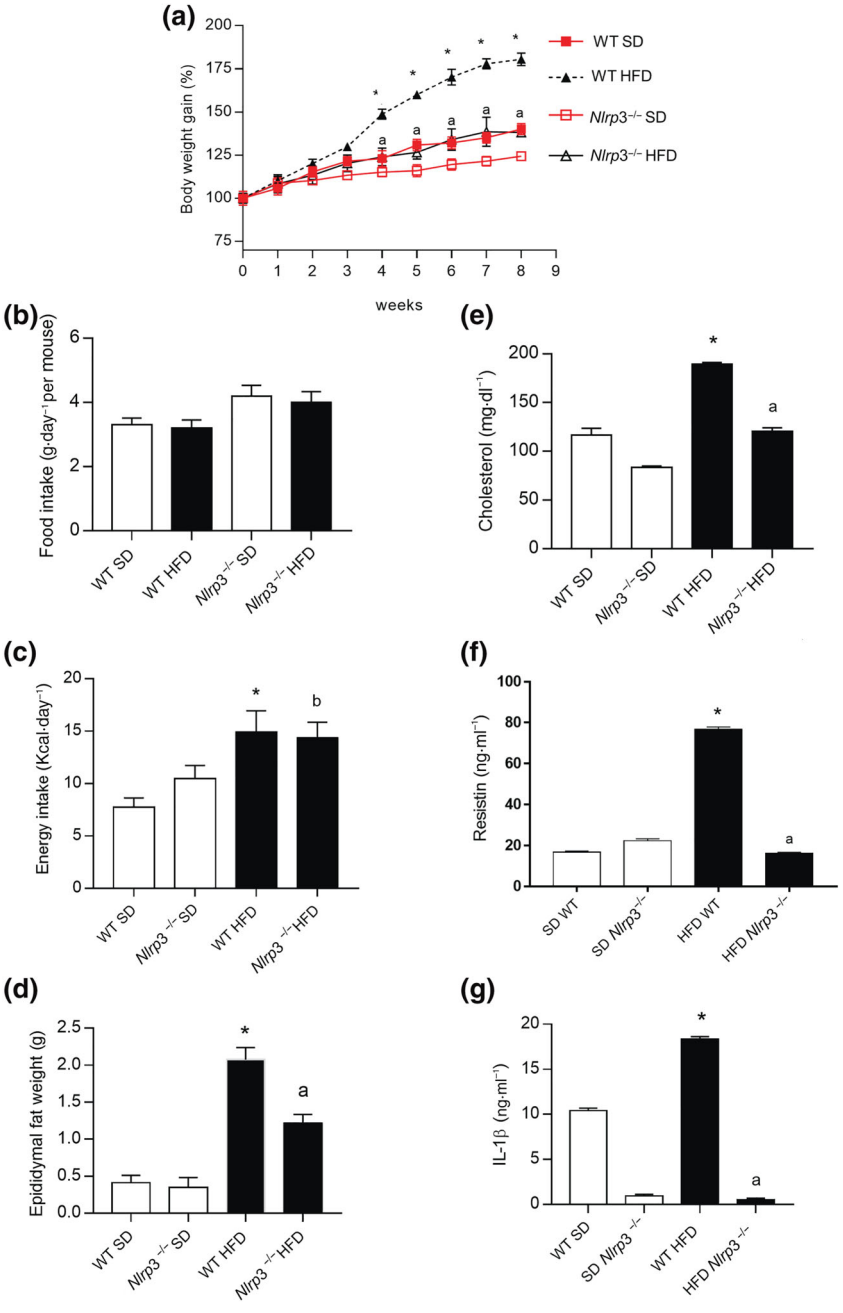

FIGURE 1 Effects of HFD on metabolic and inflammatory parameters in WT and *Nlrp3*$^{-/-}$ mice. (a) Body weight gain in WT or *Nlrp3*$^{-/-}$ mice fed with SD or HFD ($n = 10$ per group). Two-way ANOVA followed by Tukey's post hoc test results. **P* < 0.05 significant difference versus WT SD; ^{a}P < 0.05 significant difference versus WT HFD. (b) Food intake in WT or *Nlrp3*$^{-/-}$ mice fed with SD or HFD. (c) Energy intake in WT or NLRP3$^{-/-}$ mice fed with SD or HFD. (d) Epididymal fat weight in WT or *Nlrp3*$^{-/-}$ mice fed with SD or HFD. (e) Cholesterol blood levels in WT or *Nlrp3*$^{-/-}$ mice fed with SD or HFD. (f) Plasma resistin levels in SD or HFD mice. (g) Plasma IL-1β levels in SD or HFD mice ($n = 10$ per group). Kruskal–Wallis test followed by Dunn's post hoc test results: **P* < 0.05 significant difference versus WT SD; ^{a}P < 0.05 significant difference versus WT HFD; ^{b}P < 0.05 significant difference versus *Nlrp3*$^{-/-}$ SD. Abbreviations: HFD, high-fat diet; SD; standard diet; WT, wild type

caspase-recruitment domain (ASC) (AL177, Adipogen, San Diego CA, USA, RRID:AB_11181932) and rat anti-F4/80 (MCA497GA, BioRad, CA, USA, RRID:AB_323806); the secondary antibodies Alexa Fluor 488 donkey anti-rabbit IgG (A21206, Thermo Fisher Scientific, Milan, Italy, RRID:AB_2535792), and biotinylated anti-rat IgG (BA-9400, Vector, Burlingame, CA, USA, RRID:AB_2336202) plus Alexa Fluor Streptavidin 555 conjugated (Invitrogen, S32355, RRID:AB_2571525) were employed for ASC and F4/80 detection, respectively. In Figure 6, the antibodies used for ASC immunodetection were rabbit anti-ASC (Santa Cruz, sc-22514-R, RRID:AB_2174874) and Alexa Fluor 594-conjugated donkey anti-rabbit IgG antibody (Invitrogen, A-21207, RRID:AB_141637). Solvents of all used pharmacological tools, including sterile distilled water, DMSO and sterile PBS, did not produce any effect in in vitro experiments.

2.14 | Nomenclature of targets and ligands

Key protein targets and ligands in this article are hyperlinked to corresponding entries in the IUPHAR/BPS Guide to PHARMACOLOGY http://www.guidetopharmacology.org and are permanently archived in the Concise Guide to PHARMACOLOGY 2019/20 (Alexander et al., 2019).

3 | RESULTS

3.1 | NLRP3 inflammasome contributes to the development of HFD-induced obesity

To investigate the role of NLRP3 inflammasome in the onset of HFD-induced obesity, we performed experiments in mice with NLRP3 gene deletion. During the 8 weeks of HFD feeding, body weight was assessed weekly. After 8 weeks, energy intake, epididymal fat weight and cholesterol levels were examined. In addition, circulating levels of resistin, regarded as a hormone involved in glucose tolerance and insulin action (Steppan et al., 2001), were evaluated. HFD mice displayed a significant increase in body and epididymal fat weight as well as blood cholesterol levels (Figure 1a,d,e). In HFD *Nlrp3*$^{-/-}$ mice, the body weight gain and epidydimal fat, cholesterol increments and plasma and resistin levels were significantly lower, as compared with HFD wild type (WT) animals (Figure 1a,d–f). No significant differences in food intake were detected in SD and HFD WT or *Nlrp3*$^{-/-}$ mice (Figure 1b). No significant differences in energy intake were observed in HFD WT or *Nlrp3*$^{-/-}$ mice (Figure 1c). NLRP3 gene deletion did not exert any influence on metabolic parameters in SD mice, as compared with SD WT animals (Figure 1a–f). These results suggest that *Nlrp3*$^{-/-}$ mice were less susceptible to the development of HFD-induced obesity, thus highlighting the relevance of NLRP3 inflammasome pathways in the pathophysiology of obesity. Of note, obesity is also associated with the occurrence of systemic inflammation, characterized by an increase in circulating and adipose tissue levels of pro-inflammatory cytokines, including IL-1β (Figure 1g). In this context, we found that the HFD *Nlrp3*$^{-/-}$ mice displayed a significant decrease in circulating IL-1β levels, thus confirming that the observed lean HFD *Nlrp3*$^{-/-}$ phenotype resulted from a canonical inflammasome activation (Figure 1g) and that NLRP3 signalling is involved in the inflammation associated with obesity.

3.2 | HFD-induced obesity is associated with enteric NLRP3 inflammasome activation

As IL-1β release is regarded as the consequence of the activation of inflammasome pathways, we went on to investigate the activation of inflammasome signalling in colonic tissues from obese mice. In particular, we evaluated the mRNA expression of apoptosis-associated

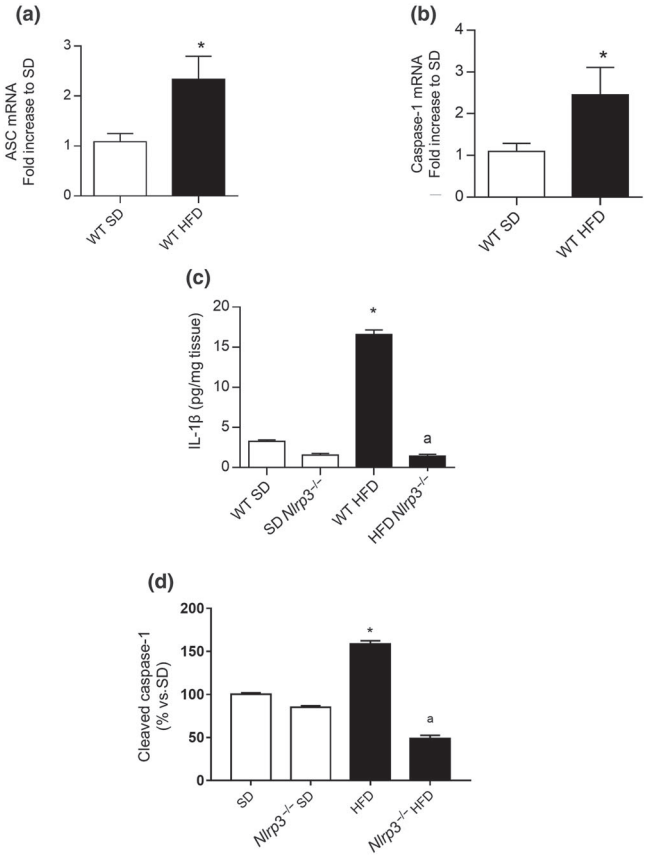

FIGURE 2 Effects of HFD on colonic inflammation in WT and *Nlrp3*$^{-/-}$ mice. (a) mRNA expression of ASC and (b) caspase-1 in colonic tissues from SD or HFD mice. (c) IL-1β levels in colonic tissues from WT or *Nlrp3*$^{-/-}$ mice fed with SD or HFD. (d) Densitometry of Western blot results for cleaved caspase-1 in SD or HFD WT and NLRP3$^{-/-}$ mice. Expression was normalized against β-actin ($n = 10$ per group). Kruskal–Wallis test followed by Dunn's post hoc test results: *$P < 0.05$ significant difference versus WT SD; $^{a}P < 0.05$ significant difference versus WT HFD. ASC, apoptosis-associated speck-like protein containing a caspase-recruitment domain; HFD, high-fat diet; IL1-β, interleukin-1-beta; SD, standard diet; WT, wild type

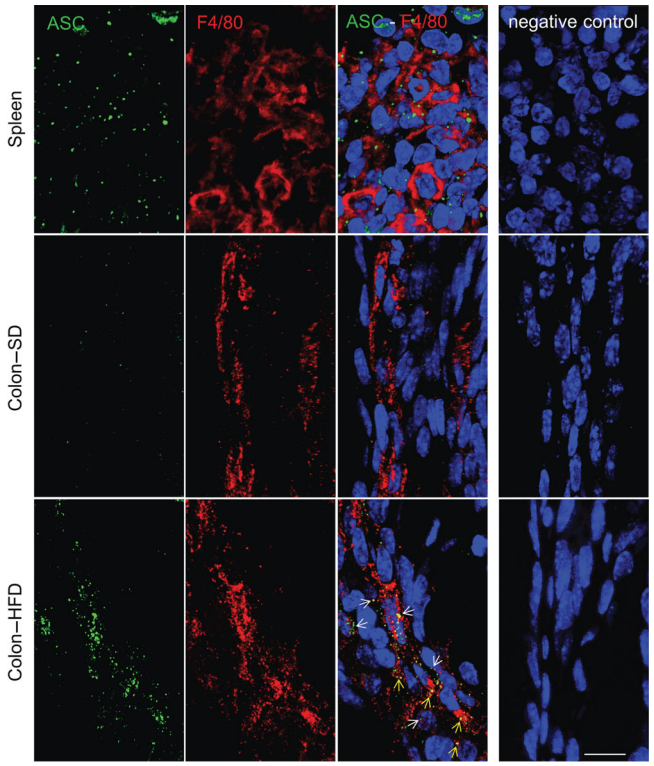

FIGURE 3 Confocal microscopy representative images of adaptor protein apoptosis-associated speck-like protein containing a caspase-recruitment domain (ASC) (green) and F4/80 (red) double immunofluorescence labelling in mouse spleen and colon. The red pulp of spleen from high-fat diet (HFD) mouse, positive control both for ASC and F4/80, shows F4/80-positive macrophages and multiple cellular (nuclear and cytoplasmic) and extracellular ASC specks. In colon sections, F4/80-positive macrophages reside in the *lamina propria*: in HFD colon, macrophages abundantly express a granular ASC positivity (green fluorescence, white arrows) often co-localized with F4/80 (yellow fluorescence, yellow arrows). Scale bar, 10 μm

speck-like protein containing a caspase recruitment domain: CARD, caspase recruitment domain; ASC, an adaptor protein required for NLRP3 oligomerization and caspase-1, the enzyme involved in the conversion of pro-IL-1 β into mature IL-1β (Lopez-Castejon et al., 2013; Strowig et al., 2012), as well as IL-1β levels in the colon from HFD mice. The results showed that ASC and caspase-1 mRNA expression along with active caspase-1 protein expression and IL-1β levels were significantly increased in colonic tissues from HFD mice, as compared with SD animals (Figure 2a–d), thus indicating the activation of canonical NLRP3 inflammasome pathway. Of note, upon inflammasome assembly, ASC within the complex can be readily visualized inside cells, including intestinal epithelial cells and immune/inflammatory cells (monocytes, macrophages, dendritic cells and T cells) (Javanmard Khameneh et al., 2019; Pellegrini et al., 2017; Rescigno, 2011) by its oligomerization and the appearance of large aggregates, designated as speck (Lopez-Castejon et al., 2013). Therefore, in order to confirm the activation of inflammasome complex in intestinal immune/inflammatory cells, we performed a double-staining immunofluorescence assay with ASC and F4/80 (macrophage marker) both in HFD mouse spleen and colon tissue slices. Our results showed macrophages in the colonic *lamina propria* with rich amount of grainy ASC-immunofluorescent aggregates localized in the nucleus (green spots) and co-localized with F4/80-positive cytoplasm (yellow spots) in colon from HFD mice (Figure 3), thus suggesting the occurrence of ASC oligomerization and consequent inflammasome activation in intestinal macrophages following HFD.

3.3 | NLRP3 activation contributes to colonic dysmotility associated with obesity, through the modulation of enteric tachykinin motor pathways

In this set of experiments, the role of NLRP3 in the alterations of colonic motility from obese mice was examined.

WT HFD animals displayed a significant decrease in stool frequency, as compared with WT SD mice (Figure 4a), confirming previous findings showing that HDF is associated with a decrease in colonic transit.

Interestingly, NLRP3 gene deletion was associated with a recovery of in vivo colonic motility as compared with HFD WT animals (Figure 4a), while no changes were observed in *Nlrp3*$^{-/-}$ mice fed with SD (Figure 4a), thus suggesting that NLRP3 activation contributes to colonic dysmotility associated with obesity.

Subsequently, because enteric substance P/NK$_1$ neuronal pathways are involved in the physiological regulation of bowel motility and undergo significant rearrangements in enteric inflammation

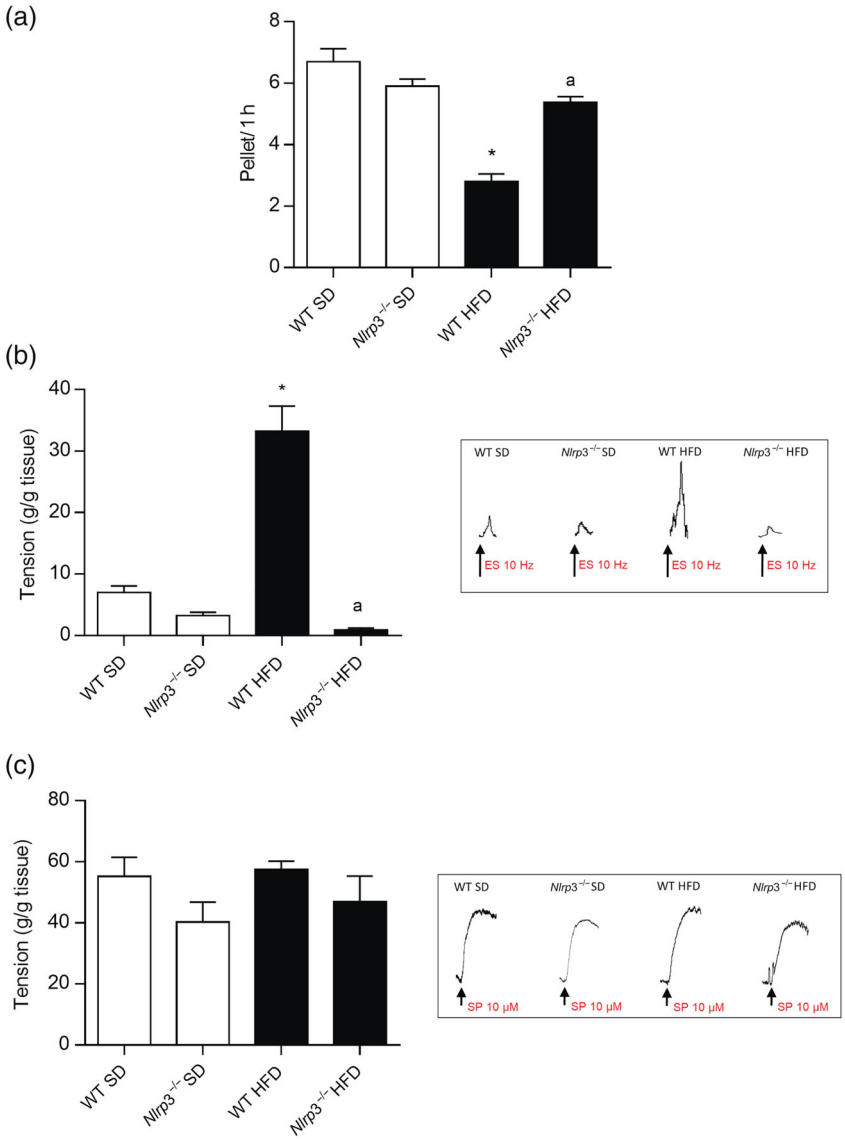

FIGURE 4 Faecal output and in vitro colonic contractile responses from SD or HFD WT and *Nlrp3*$^{-/-}$ mice. (a) Faecal output expressed as number of pellets in 1 h in WT or NLRP3$^{-/-}$ mice fed with SD or HFD (b) Effects of electrical stimulation on contractions of colonic preparations isolated from WT or *Nlrp3*$^{-/-}$ mice fed with SD or HFD. Colonic preparations were maintained in Krebs solution containing L-NAME (100 µM), guanethidine (10 µM), atropine (1 µM), GR159897 (1 µM) and SB 218795 (1 µM) to record NK_1 receptor mediated contractions. Tracings in the inset display representative contractions evoked by ES. Kruskal–Wallis test followed by Dunn's post hoc test results: *$P < 0.05$ significant difference versus WT SD; [a]$P < 0.05$ significant difference versus WT HFD. (c) Effects of exogenous SP (10 µM) on contractions of colonic preparations isolated from WT or *Nlrp3*$^{-/-}$ mice fed with SD or HFD. Colonic preparations were maintained in Krebs solution containing tetrodotoxin (1 µM). Tracings in the inset display representative contractions evoked by exogenous SP ($n = 10$ per group). Kruskal–Wallis test followed by Dunn's post hoc test results: no significant difference. ES, electrical stimulation; HFD, high-fat diet; LMMP, longitudinal muscle-myenteric plexus; SD, standard diet; SP, substance P; WT, wild type

associated with obesity (D'Antongiovanni, Pellegrini, et al., 2020), we examined the role of NLRP3 in the alterations of enteric tachykinin neurotransmission in colonic tissues from obese mice.

During equilibration, most distal colonic preparations displayed a rapid spontaneous motor activity, which was low in amplitude and generally stable throughout the experiment (data not shown). No significant differences in spontaneous motor activity were observed when comparing SD WT and *Nlrp3*$^{-/-}$ mice (mean amplitude: 2.1- and 2.3-g/g tissue, respectively) to HFD animals (mean amplitude 1.8- and 1.9-g/g tissue, respectively). Electrically evoked responses consisted of phasic contractions followed, in some cases, by after-contractions of variable amplitude. In colonic longitudinal muscle preparations maintained in Krebs solution containing L-NAME, guanethidine, GR159897, SB 218795 and atropine, electrical stimulation elicited contractile responses, which were almost completely abolished by L-732,138 or tetrodotoxin, indicating the recruitment of postganglionic tachykinin motor neurons (Figure S3).

Of note, the electrically evoked TTX-insensitive colonic contractile responses can result from the activation of TTX-resistant Na channels, including $Na_v1.6$, **$Na_v1.8$** and **$Na_v1.9$**, from TTX-resistant purinergic signalling from enteric neurons to glia cells as well as from TTX-insensitive glial stimulation (Beyak et al., 2004; Brown et al., 2016; Copel et al., 2013; Gulbransen & Sharkey, 2009; Gulbransen & Sharkey, 2012; Padilla et al., 2007; Rugiero et al., 2003; Sage et al., 2007).

Under these conditions, electrically evoked NK_1 receptor mediated colonic contractions were significantly increased in HFD mice, as compared with SD animals (Figure 4b), while no alterations were observed in the myogenic motor responses evoked by exogenous application of substance P in the presence of tetrodotoxin (Figure). Interestingly, *Nlrp3*$^{-/-}$ mice fed with HFD displayed a significant decrease in electrically evoked NK_1 receptor mediated contractions as compared with HFD WT animals (Figure 4b). Of note, electrically evoked tachykininergic colonic contractions both in control and in

HFD can result from intrinsic tachykinin motor neurons as well as from extrinsic afferents nerves and substance P interneurons (Bartho et al., 2008). In colonic longitudinal muscle preparations from HFD WT and *Nlrp3*$^{-/-}$ mice maintained in Krebs solution containing tetrodotoxin (1 μM), the contractions induced by exogenous substance P (10 μM) were comparable with those recorded in SD preparations from WT and *Nlrp3*$^{-/-}$ mice (Figure 4c). These results indicate that NLRP3 inflammasome plays a pivotal role in the pathogenesis of enteric dysmotility associated with obesity, through the modulation of enteric tachykinin neurotransmission.

Overall, these results suggest that, in the presence of obesity, an overactivation of NLRP3 inflammasome, besides shaping the immune/inflammatory responses, contributes to colonic dysmotility through the modulation of enteric tachykinin neurotransmission.

3.4 | Substance P contributes to NLRP3 activation in immune/inflammatory cells

To elucidate the mechanisms underlying the NLRP3-substance P/NK_1 interplay, we performed experiments in the LPS-primed phorbol 12-myristate 13-acetate-differentiated THP-1 cell line, an established model to investigate monocyte/macrophage functions (Chanput et al., 2014). The incubation of LPS-primed THP-1 cells with the potassium ionophore nigericin, a recognized NLRP3 inflammasome activator (Lopez-Castejon et al., 2013), induced a significant production and release of mature IL-β (Figure 5a). Such effects were abrogated upon incubation with the caspase-1 inhibitor YVAD and did not occur in ASC$^{-/-}$ THP-1 cells (Figure 5a). Interestingly, the incubation with substance P stimulated mature IL-1β release in LPS-primed THP-1 cells (Figure 5a,b). Treatment with YVAD reduced significantly the release of IL-1β induced by substance P (Figure 5b). Likewise, substance P did not evoke IL-1β release from LPS-primed ASC$^{-/-}$ THP-1 cells (Figure 5a). These results suggest that substance P promotes NLRP3 inflammasome activation and the consequent release of IL-1β in macrophage-like cells through the activation of NK_1 receptors. In support of these results, incubation of THP-1 cells with the NK_1 receptor antagonist L-732,138 at 20 and 1 μM inhibited the release of IL-1β induced by substance P (Figure 5b), while no changes in substance P-induced IL-1β were detected in the presence of NK_2 and NK_3 receptor antagonists (Figure 5b).

Of note, the incubation with GR73632 (NK_1 receptor agonist) stimulated mature IL-1β release (Figure 5b). Both nigericin and substance P induced cell death in LPS-primed THP-1 cells (Figure 5c).

3.4.1 | ASC speck detection and quantification

The activation of NLRP3 inflammasome requires oligomerization of the adaptor protein ASC that generates the formation of specks (Lopez-Castejon et al., 2013). Accordingly, in order to confirm that substance P is able to activate the NLRP3 inflammasome complex, we investigated the ability of substance P of inducing ASC oligomerization. Interestingly, the incubation of LPS-primed THP-1 cells with substance P increased significantly the numbers of ASC specks, thus suggesting the ability of substance P of promoting the oligomerization of ASC (Figure 6). Overall, these results support the view that substance P, through the stimulation of NK_1 receptors, induces NLRP3 inflammasome activation by promoting the oligomerization of ASC, the upstream inflammasome pathway.

4 | DISCUSSION

Several lines of evidence have showed that obese patients experience gastrointestinal disturbances, including delayed gastric emptying and constipation (Fysekidis et al., 2012; Mushref & Srinivasan, 2013; Rajindrajith et al., 2014). In this context, gut dysbiosis, enteric inflammation and impairments in intestinal epithelial barrier have been proposed to be involved in the onset of digestive symptoms in obesity. In particular, it has been postulated that the alterations of intestinal epithelial barrier could facilitate bacteria and their product into the mucosa and promote immune/inflammatory responses, that, in turn, may lead to alteration in the function of nerve terminals in the lamina propria, resulting in intestinal dysfunctions and obesity (Antonioli, D'Antongiovanni, et al., 2020; Raybould, 2012). Indeed, though Reichardt et al. (2013) reported no signs of enteric inflammation or impaired intestinal barrier in obese mice fed with HFD for 12 weeks (Reichardt et al., 2013), most of preclinical studies have shown that mice fed with HFD for 8 weeks are characterized by neurochemical and functional changes throughout the digestive tract, along with the gut dysbiosis, enteric inflammation and impairments of intestinal epithelial barrier that could contribute to bowel dysfunctions (Antonioli et al., 2019; Antonioli, D'Antongiovanni, et al., 2020; Ding et al., 2010; Lam et al., 2012; Raybould, 2012; Stenman et al., 2012). The opposite findings in the study by Reichardt et al. (2013) could be ascribed to different animal facility condition that could alter gut microbiota and in turn the immune/inflammatory responses associated with HFD. In addition, after 8 weeks, the supplementation with HFD might also trigger unknown compensatory bacteria-immune mechanisms with consequent decreased immune/inflammatory responses and restored intestinal epithelial barrier integrity at 12 weeks.

Of note, gut dysbiosis, enteric inflammation and altered intestinal epithelial barrier have been found to represent early events in obese mice (starting from second week of diet) that could contribute to bowel motor disturbances (Ding et al., 2010; Lam et al., 2012).

Indeed, the murine model of HFD-induced obesity is characterized by an impairment of colonic excitatory tachykinin neurotransmission, driven mainly by enteric inflammation, as corroborated by the evidence showing that the depletion of intestinal macrophages determined a normalization of colonic tachykininergic contractile activity in HFD mice (Antonioli et al., 2019). Based on this background, the present study was designed to elucidate the molecular mechanisms underlying the interplay between intestinal immune/inflammatory responses and enteric remodelling in the murine

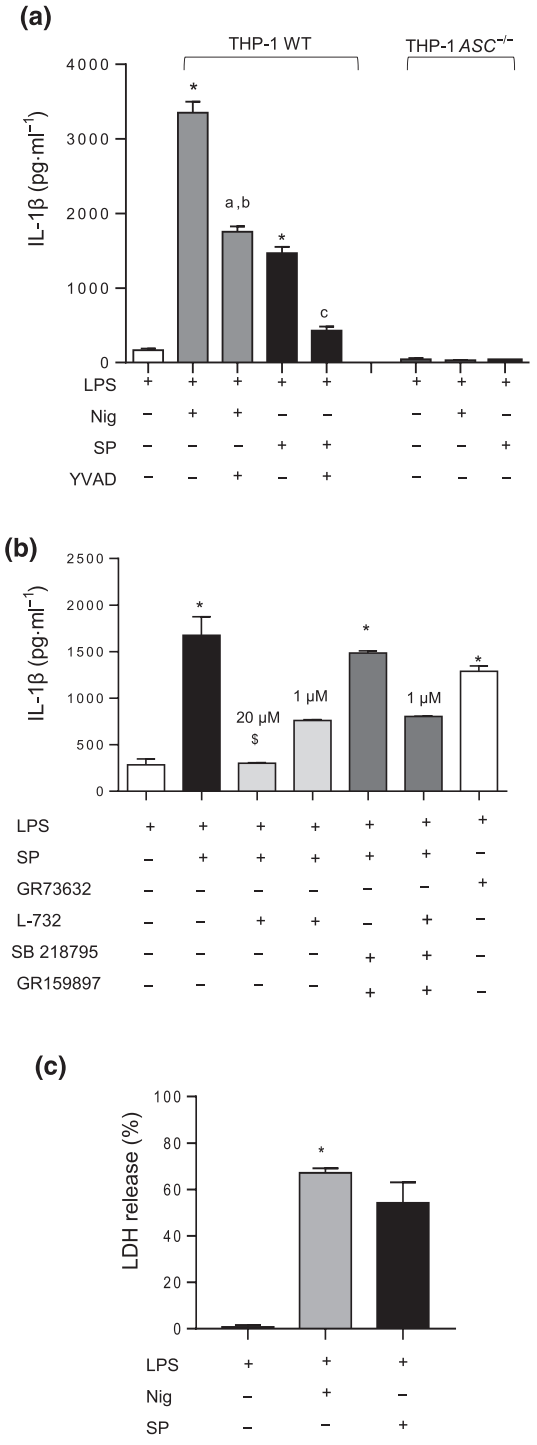

FIGURE 5 Effects of substance P (SP) on NLRP3 inflammasome signalling in THP-1 cells. (a) IL-1β levels in thesupernatants of LPS-primed THP-1 cells treated with Nig or SP in the presence or in the absence of YVAD, or in LPS-primed *ASC*$^{-/-}$ THP-1 cells treated with Nig or SP ($n = 6$ experiments). (b) IL-1β levels in the supernatants of LPS-primed THP-1 cells treated with SP or GR73632 (NK1 receptor agonist) in the presence or in the absence of GR159897 (NK2 receptor antagonist) and SB 218795 (NK3 receptor antagonist) and L-732,138 (NK1 receptor antagonist) ($n = 6$ experiments). (c) LDH release in the supernatants of LPS-primed THP-1 cells treated with Nig or SP ($n = 6$ experiments).One-way ANOVA followed by Tukey's post hoc test results: $^{*}P < .05$ significant difference versus LPS-primed THP-1; $^{a}P < 0.05$, significant difference versus LPS-primed THP-1 treated with Nig; $^{b}P < 0.05$,significant difference versus LPS-primed THP-1; $^{c}P < 0.05$, significant difference versus LPS-primed THP-1 treated with SP; $^{\$}P < 0.05$,significant difference versus LPS-primed THP-1 treated with SP; $^{\#}P < 0.05$,significant difference versus LPS-primed THP-1 treated with SP). ASC, apoptosis-associated speck-like protein containing acaspase-recruitment domain; IL1-β, interleukin-1-beta; LDH, lactate dehydrogenase; LPS, lipopolysaccharide; Nig, nigericin; SP, substance P; THP-1, wild type human monocytic cell line

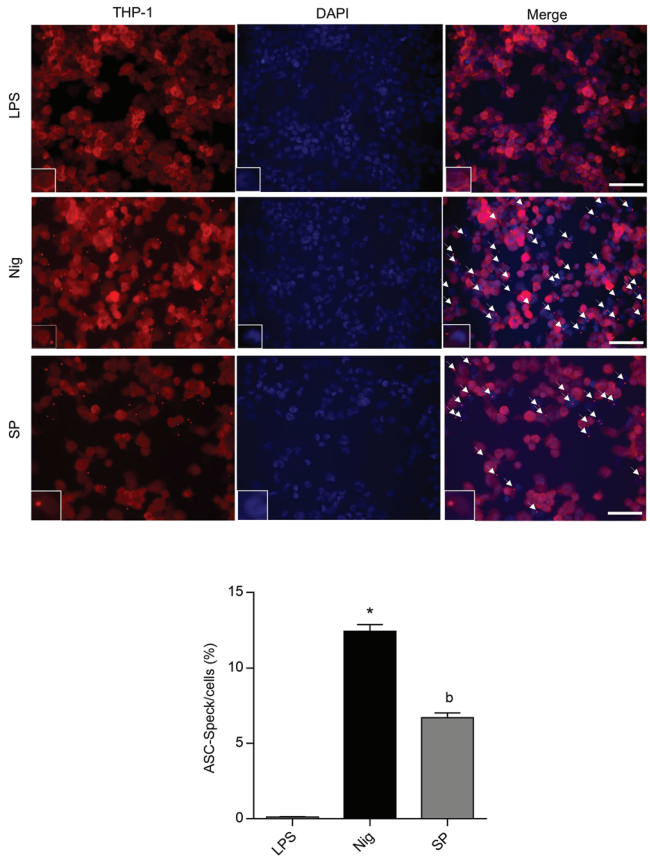

FIGURE 6 Immunofluorescence analysis of ASC in THP-1 cells. Representative immunofluorescence images and analysis of ASC expression in LPS-primed (1 g·ml^{-1}, 4 h) THP-1 treated with Nig (10 μM, 1 h) or SP (10 μM, 2 h). The number of ASC specks was quantified and expressed as the percentage of specks per cell number. ($n = 6$ experiments). One-way ANOVA followed by Tukey's post hoc test results: $^{*}P < 0.05$, significant difference versus LPS-primed THP-1 cells; $^{a}P < 0.05$, significant difference versus LPS-primed THP-1 treated with Nig; $^{b}P < 0.05$, significant difference versus LPS-primed THP-1. Scale bar = 50 μm. ASC, apoptosis-associated speck-like protein containing a caspase-recruitment domain; Nig, Nigericin; SP, substance P; THP-1, wild type human monocytic cell line

model of HFD-induced obesity. In particular, we focused our attention on the NLRP3 inflammasome complex, based on growing evidence supporting its involvement in shaping immune/inflammatory responses in several disorders, including obesity, atherosclerosis, type 2 diabetes mellitus, gout and bowel inflammation (Broderick et al., 2015; De Nardo & Latz, 2011; Pellegrini et al., 2017). Under these pathological conditions, the NLRP3 inflammasome, a key sensor of cellular stress involved in IL-1β release, takes part actively in the immune/inflammatory responses (Pellegrini et al., 2017).

Taken together, the results of the present study shed light on the involvement of NLRP3 in the phlogistic process associated with diet-induced obesity, providing novel and intriguing evidence about the role of this enzyme complex as an immune sentinel, which takes a significant part in driving the rearrangement of enteric tachykinin pathways in HFD-fed animals. In particular, our study presents the following points of novelty: (1) NLRP3 inflammasome is involved in several pathophysiological processes associated with obesity, such as metabolic and inflammatory parameters, and (2) NLRP3 signalling regulates the interplay between intestinal immune/inflammatory cells and enteric substance P/NK_1 pathways contributing to enteric dysmotility associated with obesity.

In line with previous studies, we observed that WT mice fed with HFD displayed a significant increment of body and epididymal fat weight, blood cholesterol levels, circulating resistin levels and circulating IL-1β levels, thus confirming the existence of a link between a hyperlipidaemic diet intake with an excessive fat accumulation, alterations of metabolic parameters and systemic inflammation (Antonioli et al., 2017, 2019). Interestingly, such detrimental effects, associated with HFD, were not observed in NLRP3 deficient animals, thus corroborating previous preclinical and clinical evidence describing the relevance of NLRP3 inflammasome in the pathophysiology of obesity and related inflammation (Donath et al., 2010; Lee et al., 2013; Pavillard et al., 2017; Rheinheimer et al., 2017; Steppan et al., 2001; Stienstra et al., 2011; Vandanmagsar et al., 2011). In particular, NLRP3 gene deletion reduced significantly resistin levels in plasma from HFD WT mice, suggesting also a role of NLRP3 in the onset of insulin resistance.

As a first step, we designed a set of experiments aimed at investigating the role of NLRP3 inflammasome in the enteric immune/

inflammatory responses associated with obesity. For this purpose, we evaluated the mRNA expression of ASC and caspase-1 as well as active caspase-1 protein expression in colonic tissues from HFD mice, assaying also in parallel tissue IL-β levels. We observed a significant increase both in ASC and caspase-1 mRNA and in active caspase-1 protein expression along with in IL-1β tissue levels in HFD mice, thus indicating the activation of the well-established pattern of canonical inflammasome pathway (Pellegrini et al., 2017). Of note, HFD exposure in mice with NLRP3 gene deletion was associated with a decrease in the cleavage of caspase-1 in its active form along with lower levels of IL-1β as compared with WT HFD animals, providing the first demonstration that NLRP3 inflammasome activation contributes to trigger immune/inflammatory responses in this model of obese mouse.

Subsequently, a double-staining immunofluorescence analysis was performed to investigate ASC oligomerization, reflecting an active status of the inflammasome, at level of F4/80-positive bowel macrophages. In these experiments, appreciable amount of ASC dots was observed in macrophages within the *lamina propria* of colonic tissues from HFD mice, indicating a polarization towards a pro-inflammatory phenotype of these cells (Pelegrin & Surprenant, 2009). Of note, these data represent the first clear evidence of double-immunostaining of ASC specks in F4/80-positive macrophages available in paraffin tissue samples of spleen and colon. Despite previous studies reported an increase in pro-inflammatory cytokines sustained by the presence of M1 macrophages in the digestive tract of HFD mice (Antonioli et al., 2019; Luck et al., 2015), our study provides the first evidence of a role of NLRP3 inflammasome in driving such phenotypic pro-inflammatory shift. Thus, based on these findings, the concept arises of a pivotal role of NLRP3 inflammasome signalling in driving enteric inflammation in obese mice, mainly via IL-1β release. A number of studies have reported the presence of a low-grade inflammatory status in the gut as a driver for the induction of morpho-functional changes in enteric nerves, glia, interstitial cells of Cajal or smooth muscle cells, with consequent alterations of digestive motor activity (Antonioli et al., 2019; Antonioli, D'Antongiovanni, et al., 2020; Khan & Collins, 2006). In this context, intestinal macrophages were shown to participate actively to the onset of such bowel motor dysfunctions. Indeed, the depletion of intestinal macrophages in HFD mice, beyond determining an improvement of colonic inflammation, induced also a normalization of the abnormal tachykininergic contractions observed in obese animals (Antonioli et al., 2019). Of note, previous studies, conducted on human colonic epithelial cell lines or intestinal tissues from patients with inflammatory bowel diseases, identified IL-1β as the pivotal driver in the onset of altered tachykinin transmission, resulting in an enhanced substance P release and increased NK_1 receptor expression (Goode et al., 2003; Margolis & Gershon, 2009). Interestingly, the authors reported that the occurrence of a vicious circle, linking substance P/NK_1 signalling with IL-1β release, is the basis explaining the maintenance of altered neurogenic/immune processes (Goode et al., 2003; Margolis & Gershon, 2009). In order to verify the involvement of NLRP3 inflammasome in sustaining the tachykininergic/IL-1β interplay in colonic tissues of obese animals, we designed specific sets of experiments in NLRP3 deficient mice fed with HFD. Under this experimental condition, we observed that the genetic ablation of NLRP3 reduced IL-1β levels in colonic tissues from HFD mice. In addition, in NLRP3 deficient animals, HFD intake failed to induce the functional alterations of colonic tachykinin pathways typically observed in the obese WT animals fed with HFD, resulting in a recovery of in vivo colonic transit. In this setting, it is noteworthy that the overall colonic propulsive motility is the resultant of an integrated combination of circular and longitudinal smooth muscle contractions regulated by both excitatory and inhibitory neurotransmitter pathways (Bornstein et al., 2004). In addition, it is well documented that an increase in colonic tachykininergic contractions characterized by a marked substance P release is associated with alterations of peristaltic movements with consequent decrease of colonic propulsive activity. Therefore, it is conceivable that the recovery of in vivo colonic transit following NLRP3 gene deletion could be ascribable to the normalization of excitatory tachykininergic colonic contractions, markedly increased in obese animals. In parallel, NLRP3 depletion, counteracting the enteric inflammatory responses, could determine an amelioration of colonic contractions (Goverse et al., 2016).

However, an integrated assessment of the patterns of in vitro excitatory and inhibitory colonic motor pathways in HFD *Nlrp3*$^{-/-}$ mice remains to be clarified and could represent the logical continuation in this research topic.

Taken together, these results provide convincing evidence that, in the setting of obesity, the activation of colonic NLRP3 inflammasome signalling, promoting a massive release of IL-1β, determines an impairment of enteric tachykinin neurotransmission characterized by an enhanced substance P release, that, in turn, contributes to colonic dysmotility. Of note, a previous study, performed in a murine model of postoperative ileus, corroborates our hypothesis, because, despite not focusing the attention on tachykinin pathways, it reported that treatment with **anakinra**, an IL-1β receptor antagonist, counteracted the bowel dysmotility associated with this pathological condition, thus suggesting an involvement of inflammasome pathways in the onset of bowel motor dysfunctions in the post-operative ileus model (Stoffels et al., 2014).

However, we cannot rule out that NLRP3 could also contribute to enteric inflammation and bowel dysmotility by activating other cellular and molecular signalling independently on of its canonical-caspase-1 dependent activation.

In an attempt of characterizing the molecular mechanisms underlying the interplay between NLRP3 inflammasome and enteric substance P/NK_1 neuronal pathways, we performed a series of in vitro experiments on phorbol 12-myristate 13-acetate-differentiated THP-1 cells, an established cell model suitable for investigating monocyte/macrophage inflammatory responses (Chanput et al., 2014). Of note, human monocytes and macrophages are known to express NK_1 receptors (Ho et al., 1997). In our experiments, THP-1 cells were incubated with LPS, which beside being a well-recognized activator of the first step of NLRP3 signalling represents also a hallmark of altered intestinal permeability, a condition typically observed both in the

murine model of HFD-induced obesity and obese patients (Dalby et al., 2018; Troseid et al., 2013). THP-1 cells were treated with substance P to examine its effect on NLRP3 inflammasome. These results showed for the first time, a stimulant effect of substance P on NLRP3 inflammasome, with a consequent increase in IL-1β release. The existence of a substance P/NLRP3 axis was corroborated by further sets of experiments on $ASC^{-/-}$ THP-1 cells or WT cells pretreated with a caspase-1 inhibitor or a selective NK_1 receptor antagonist, in which the stimulant effect of substance P on IL-1β release no longer occurred. These findings are in line with previous papers showing that substance P in synergy with LPS induced IL-1β release in several cell types, including human peripheral mononuclear cells, astrocytes and microglia (Cuesta et al., 2002; Lieb et al., 1996; Martin et al., 1992; Martin et al., 1993). However, these studies did not investigate the possible involvement of NLRP3 inflammasome complex.

Taken together, these findings support the evidence of a direct stimulant effect of substance P on NLRP3 inflammasome/IL-1β pathways. Thus, based on these observations, it is conceivable that, in the presence of obesity, an increase in colonic NLRP3-induced IL-1β levels contributes to an enhanced substance P release from myenteric neurons as well as extrinsic afferents nerves and substance P interneurons (Bartho et al., 2008). Such increment, beyond playing a critical role in the altered enteric tachykinin neurotransmission, seems to trigger the activation of NLRP3 inflammasome/IL-1β axis in macrophages through the recruitment of NK_1 receptors.

5 | CONCLUSIONS

In conclusion, the present study provides convincing evidence supporting a role of NLRP3 inflammasome complex as a regulatory hub linking the intestinal innate immune/inflammatory cells with the enteric substance P/NK_1 neuronal pathways, taking a relevant part both in the pathophysiology of inflammatory process and the enteric motor disorders associated with obesity. Based on this knowledge, the NLRP3 inflammasome may represent an interesting molecular target for the development of novel pharmacological approaches aimed at managing the inflammatory and enteric motor dysfunctions associated with obesity.

ACKNOWLEDGEMENT

This research was supported by the PRA_2020_46 granted by the University of Pisa.

AUTHOR CONTRIBUTIONS

CP and MF designed the study and write original draft preparation. LB, VC, PPR, AN, FG, VDA, CS, CI and GLC collected and analysed the data. RC, MCG, MN and NB interpreted the data. PP, GH, CB and LA co-authored the writing of the manuscript and edited the manuscript. All authors read and approved the final manuscript.

CONFLICT OF INTEREST

The authors declare no conflict of interest.

DECLARATION OF TRANSPARENCY AND SCIENTIFIC RIGOUR

This Declaration acknowledges that this paper adheres to the principles for transparent reporting and scientific rigour of preclinical research as stated in the BJP guidelines for Natural Product Research, Design and Analysis, Immunoblotting and Immunochemistry, and Animal Experimentation, and as recommended by funding agencies, publishers and other organizations engaged with supporting research.

DATA AVAILABILITY STATEMENT

Data are available upon request from the authors.

REFERENCES

Alexander, S. P. H., Christopoulos, A., Davenport, A. P., Kelly, E., Mathie, A., Peters, J. A., Veale, E. L., Armstrong, J. F., Faccenda, E., Harding, S. D., Pawson, A. J., Sharman, J. L., Southan, C., Davies, J. A., & CGTP collaborators. (2019). The Concise Guide to PHARMACOLOGY 2019/20: G protein-coupled receptors. *British Journal of Pharmacology*, *176*(Suppl 1), S21–S141. https://doi.org/10.1111/bph.14748

Alexander, S. P. H., Roberts, R. E., Broughton, B. R. S., Sobey, C. G., George, C. H., Stanford, S. C., Cirino, G., Docherty, J. R., Giembycz, M. A., Hoyer, D., Insel, P. A., Izzo, A. A., Ji, Y., MacEwan, D. J., Mangum, J., Wonnacott, S., & Ahluwalia, A. (2018). Goals and practicalities of immunoblotting and immunohistochemistry: A guide for submission to the British Journal of Pharmacology. *British Journal of Pharmacology*, *175*, 407–411. https://doi.org/10.1111/bph.14112

Andersen, C. J., Murphy, K. E., & Fernandez, M. L. (2016). Impact of obesity and metabolic syndrome on immunity. *Advances in Nutrition*, *7*, 66–75. https://doi.org/10.3945/an.115.010207

Antonioli, L., Caputi, V., Fornai, M., Pellegrini, C., Gentile, D., Giron, M. C., Orso, G., Bernardini, N., Segnani, C., Ippolito, C., Csóka, B., Haskó, G., Németh, Z. H., Scarpignato, C., Blandizzi, C., & Colucci, R. (2019). Interplay between colonic inflammation and tachykininergic pathways in the onset of colonic dysmotility in a mouse model of diet-induced obesity. *International Journal of Obesity*, *43*, 331–343. https://doi.org/10.1038/s41366-018-0166-2

Antonioli, L., D'Antongiovanni, V., Pellegrini, C., Fornai, M., Benvenuti, L., Carlo, A., den Wijngaard, R., Caputi, V., Cerantola, S., Giron, M. C., Németh, Z. H., Haskó, G., Blandizzi, C., & Colucci, R. (2020). Colonic dysmotility associated with high-fat diet-induced obesity: Role of enteric glia. *FASEB Journal: Official Publication of the Federation of American Societies for Experimental Biology*, *34*, 5512–5524. https://doi.org/10.1096/fj.201901844R

Antonioli, L., Fornai, M., Colucci, R., Awwad, O., Ghisu, N., Tuccori, M., del Tacca, M., & Blandizzi, C. (2011). Differential recruitment of high affinity A1 and A2A adenosine receptors in the control of colonic neuromuscular function in experimental colitis. *European Journal of Pharmacology*, *650*, 639–649. https://doi.org/10.1016/j.ejphar.2010.10.041

Antonioli, L., Moriconi, D., Masi, S., Bottazzo, D., Pellegrini, C., Fornai, M., Anselmino, M., Ferrannini, E., Blandizzi, C., Taddei, S., & Nannipieri, M. (2020). Differential impact of weight loss and glycemic control on inflammasome signaling. *Obesity*, *28*, 609–615. https://doi.org/10.1002/oby.22734

Antonioli, L., Pellegrini, C., Fornai, M., Tirotta, E., Gentile, D., Benvenuti, L., Giron, M. C., Caputi, V., Marsilio, I., Orso, G., Bernardini, N., Segnani, C., Ippolito, C., Csóka, B., Németh, Z. H., Haskó, G., Scarpignato, C., Blandizzi, C., & Colucci, R. (2017). Colonic motor dysfunctions in a mouse model of high-fat diet-induced obesity: An involvement of A2B adenosine receptors. *Purinergic Signalling*, *13*, 497–510. https://doi.org/10.1007/s11302-017-9577-0

Bartho, L., Benko, R., Holzer-Petsche, U., Holzer, P., Undi, S., & Wolf, M. (2008). Role of extrinsic afferent neurons in gastrointestinal motility. *European Review for Medical and Pharmacological Sciences*, *12*(Suppl 1), 21–31.

Beyak, M. J., Ramji, N., Krol, K. M., Kawaja, M. D., & Vanner, S. J. (2004). Two TTX-resistant Na+ currents in mouse colonic dorsal root ganglia neurons and their role in colitis-induced hyperexcitability. *American Journal of Physiology. Gastrointestinal and Liver Physiology*, *287*(4), G845–G855. https://doi.org/10.1152/ajpgi.00154.2004

Bornstein, J. C., Costa, M., & Grider, J. R. (2004). Enteric motor and interneuronal circuits controlling motility. *Neurogastroenterology and Motility: The Official Journal of the European Gastrointestinal Motility Society*, *16*(Suppl 1), 34–38. https://doi.org/10.1111/j.1743-3150.2004.00472.x

Bremner, J. D., Innis, R. B., Southwick, S. M., Staib, L., Zoghbi, S., & Charney, D. S. (2000). Decreased benzodiazepine receptor binding in prefrontal cortex in combat-related posttraumatic stress disorder. *The American Journal of Psychiatry*, *157*(7), 1120–1126. https://doi.org/10.1176/appi.ajp.157.7.1120

Broderick, L., De Nardo, D., Franklin, B. S., Hoffman, H. M., & Latz, E. (2015). The inflammasomes and autoinflammatory syndromes. *Annual Review of Pathology*, *10*, 395–424. https://doi.org/10.1146/annurev-pathol-012414-040431

Brown, I. A., McClain, J. L., Watson, R. E., Patel, B. A., & Gulbransen, B. D. (2016). Enteric glia mediate neuron death in colitis through purinergic pathways that require connexin-43 and nitric oxide. *Cellular and Molecular Gastroenterology and Hepatology*, *2*(1), 77–91. https://doi.org/10.1016/j.jcmgh.2015.08.007

Casadesus, G., Shukitt-Hale, B., & Joseph, J. A. (2001). Automated measurement of age-related changes in the locomotor response to environmental novelty and home-cage activity. *Mechanisms of Ageing and Development*, *122*, 1887–1897. https://doi.org/10.1016/S0047-6374(01)00324-4

Chanput, W., Mes, J. J., & Wichers, H. J. (2014). THP-1 cell line: An in vitro cell model for immune modulation approach. *International Immunopharmacology*, *23*(1), 37–45. https://doi.org/10.1016/j.intimp.2014.08.002

Copel, C., Clerc, N., Osorio, N., Delmas, P., & Mazet, B. (2013). The Nav1.9 channel regulates colonic motility in mice. *Frontiers in Neuroscience*, *7*(58), 1–8.

Csoka, B., Toro, G., Vindeirinho, J., Varga, Z. V., Koscso, B., Nemeth, Z. H., Kókai, E., Antonioli, L., Suleiman, M., Marchetti, P., Cseri, K., Deák, Á., Virág, L., Pacher, P., Bai, P., & Haskó, G. (2017). A2A adenosine receptors control pancreatic dysfunction in high-fat-diet-induced obesity. *FASEB Journal: Official Publication of the Federation of American Societies for Experimental Biology*, *31*(11), 4985–4997. https://doi.org/10.1096/fj.201700398R

Cuesta, M. C., Quintero, L., Pons, H., & Suarez-Roca, H. (2002). Substance P and calcitonin gene-related peptide increase IL-1 beta, IL-6 and TNF alpha secretion from human peripheral blood mononuclear cells. *Neurochemistry International*, *40*(4), 301–306. https://doi.org/10.1016/S0197-0186(01)00094-8

Cunin, P., Caillon, A., Corvaisier, M., Garo, E., Scotet, M., Blanchard, S., Delneste, Y., & Jeannin, P. (2011). The tachykinins substance P and hemokinin-1 favor the generation of human memory Th17 cells by inducing IL-1beta, IL-23, and TNF-like 1A expression by monocytes. *Journal of Immunology*, *186*(7), 4175–4182. https://doi.org/10.4049/jimmunol.1002535

Curtis, M. J., Alexander, S., Cirino, G., Docherty, J. R., George, C. H., Giembycz, M. A., Hoyer, D., Insel, P. A., Izzo, A. A., Ji, Y., MacEwan, D. J., Sobey, C. G., Stanford, S. C., Teixeira, M. M., Wonnacott, S., & Ahluwalia, A. (2018). Experimental design and analysis and their reporting II: Updated and simplified guidance for authors and peer reviewers. *British Journal of Pharmacology*, *175*, 987–993. https://doi.org/10.1111/bph.14153

Dalby, M. J., Aviello, G., Ross, A. W., Walker, A. W., Barrett, P., & Morgan, P. J. (2018). Diet induced obesity is independent of metabolic endotoxemia and TLR4 signalling, but markedly increases hypothalamic expression of the acute phase protein, SerpinA3N. *Scientific Reports*, *8*(1), 15648. https://doi.org/10.1038/s41598-018-33928-4

D'Antongiovanni, V., Benvenuti, L., Fornai, M., Pellegrini, C., van den Wijngaard, R., Cerantola, S., Giron, M. C., Caputi, V., Colucci, R., Haskó, G., Németh, Z. H., Blandizzi, C., & Antonioli, L. (2020). Glial A2B adenosine receptors modulate abnormal tachykininergic responses and prevent enteric inflammation associated with high fat diet-induced obesity. *Cell*, *9*(5), 1245.

D'Antongiovanni, V., Pellegrini, C., Fornai, M., Colucci, R., Blandizzi, C., Antonioli, L., & Bernardini, N. (2020). Intestinal epithelial barrier and neuromuscular compartment in health and disease. *World Journal of Gastroenterology*, *26*(14), 1564–1579. https://doi.org/10.3748/wjg.v26.i14.1564

De Nardo, D., & Latz, E. (2011). NLRP3 inflammasomes link inflammation and metabolic disease. *Trends in Immunology*, *32*, 373–379. https://doi.org/10.1016/j.it.2011.05.004

Ding, S., Chi, M. M., Scull, B. P., Rigby, R., Schwerbrock, N. M., Magness, S., Jobin, C., & Lund, P. K. (2010). High-fat diet: Bacteria interactions promote intestinal inflammation which precedes and correlates with obesity and insulin resistance in mouse. *PLoS ONE*, *5*(8), e12191. https://doi.org/10.1371/journal.pone.0012191

Donath, M. Y., Boni-Schnetzler, M., Ellingsgaard, H., Halban, P. A., & Ehses, J. A. (2010). Cytokine production by islets in health and diabetes: Cellular origin, regulation and function. *Trends in Endocrinology and Metabolism: TEM*, *21*(5), 261–267. https://doi.org/10.1016/j.tem.2009.12.010

Fazzini, A., D'Antongiovanni, V., Giusti, L., Da Valle, Y., Ciregia, F., Piano, I., Caputo, A., D'Ursi, A. M., Gargini, C., Lucacchini, A., & Mazzoni, M. R. (2014). Altered protease-activated receptor-1 expression and signaling in a malignant pleural mesothelioma cell line, NCI-H28, with homozygous deletion of the beta-catenin gene. *PLoS ONE*, *9*(3), e111550. https://doi.org/10.1371/journal.pone.0111550

Fuchs, F., Damm, J., Gerstberger, R., Roth, J., & Rummel, C. (2013). Activation of the inflammatory transcription factor nuclear factor interleukin-6 during inflammatory and psychological stress in the brain. *Journal of Neuroinflammation*, *10*(140), 1–16.

Fysekidis, M., Bouchoucha, M., Bihan, H., Reach, G., Benamouzig, R., & Catheline, J. M. (2012). Prevalence and co-occurrence of upper and lower functional gastrointestinal symptoms in patients eligible for bariatric surgery. *Obesity Surgery*, *22*, 403–410. https://doi.org/10.1007/s11695-011-0396-z

Gallagher, T. K., Geoghegan, J. G., Baird, A. W., & Winter, D. C. (2007). Implications of altered gastrointestinal motility in obesity. *Obesity Surgery*, *17*, 1399–1407. https://doi.org/10.1007/s11695-007-9221-0

Goode, T., O'Connor, T., Hopkins, A., Moriarty, D., O'Sullivan, G. C., Collins, J. K., O'Donoghue, D., Baird, A. W., O'Connell, J., & Shanahan, F. (2003). Neurokinin-1 receptor (NK-1R) expression is induced in human colonic epithelial cells by proinflammatory cytokines and mediates proliferation in response to substance P. *Journal of Cellular Physiology*, *197*, 30–41. https://doi.org/10.1002/jcp.10234

Goverse, G., Stakenborg, M., & Matteoli, G. (2016). The intestinal cholinergic anti-inflammatory pathway. *The Journal of Physiology*, *594*, 5771–5780. https://doi.org/10.1113/JP271537

Gulbransen, B. D., & Sharkey, K. A. (2009). Purinergic neuron-to-glia signaling in the enteric nervous system. *Gastroenterology*, *136*, 1349–1358. https://doi.org/10.1053/j.gastro.2008.12.058

Gulbransen, B. D., & Sharkey, K. A. (2012). Novel functional roles for enteric glia in the gastrointestinal tract. *Nature Reviews. Gastroenterology & Hepatology*, *9*, 625–632. https://doi.org/10.1038/nrgastro.2012.138

Ho, W. Z., Lai, J. P., Zhu, X. H., Uvaydova, M., & Douglas, S. D. (1997). Human monocytes and macrophages express substance P and neurokinin-1 receptor. *Journal of Immunology*, *159*(11), 5654–5660.

Hume, D. A., Perry, V. H., & Gordon, S. (1984). The mononuclear phagocyte system of the mouse defined by immunohistochemical localisation of antigen F4/80: Macrophages associated with epithelia. *The Anatomical Record*, *210*, 503–512. https://doi.org/10.1002/ar.1092100311

Ippolito, C., Colucci, R., Segnani, C., Errede, M., Girolamo, F., Virgintino, D., Dolfi, A., Tirotta, E., Buccianti, P., di Candio, G., Campani, D., Castagna, M., Bassotti, G., Villanacci, V., Blandizzi, C., & Bernardini, N. (2016). Fibrotic and vascular remodelling of colonic wall in patients with active ulcerative colitis. *Journal of Crohn's & Colitis*, *10*, 1194–1204. https://doi.org/10.1093/ecco-jcc/jjw076

Javanmard Khameneh, H., Leong, K. W. K., Mencarelli, A., Vacca, M., Mambwe, B., Neo, K., Tay, A., Zolezzi, F., Lee, B., & Mortellaro, A. (2019). The Inflammasome adaptor ASC intrinsically limits CD4(+) T-cell proliferation to help maintain intestinal homeostasis. *Frontiers in Immunology*, *10*, 1–15, 1566. https://doi.org/10.3389/fimmu.2019.01566

Kataoka, N., Shima, Y., Nakajima, K., & Nakamura, K. (2020). A central master driver of psychosocial stress responses in the rat. *Science*, *367*, 1105–1112. https://doi.org/10.1126/science.aaz4639

Khan, W. I., & Collins, S. M. (2006). Gut motor function: Immunological control in enteric infection and inflammation. *Clinical and Experimental Immunology*, *143*, 389–397. https://doi.org/10.1111/j.1365-2249.2005.02979.x

Kim, K. A., Gu, W., Lee, I. A., Joh, E. H., & Kim, D. H. (2012). High fat diet-induced gut microbiota exacerbates inflammation and obesity in mice via the TLR4 signaling pathway. *PLoS ONE*, *7*, e47713. https://doi.org/10.1371/journal.pone.0047713

Lai, J. P., Ho, W. Z., Kilpatrick, L. E., Wang, X., Tuluc, F., Korchak, H. M., & Douglas, S. D. (2006). Full-length and truncated neurokinin-1 receptor expression and function during monocyte/macrophage differentiation. *Proceedings of the National Academy of Sciences of the United States of America*, *103*(20), 7771–7776. https://doi.org/10.1073/pnas.0602563103

Lam, Y. Y., Ha, C. W., Campbell, C. R., Mitchell, A. J., Dinudom, A., Oscarsson, J., Cook, D. I., Hunt, N. H., Caterson, I. D., Holmes, A. J., & Storlien, L. H. (2012). Increased gut permeability and microbiota change associate with mesenteric fat inflammation and metabolic dysfunction in diet-induced obese mice. *PLoS ONE*, *7*, e34233. https://doi.org/10.1371/journal.pone.0034233

Lee, H. M., Kim, J. J., Kim, H. J., Shong, M., Ku, B. J., & Jo, E. K. (2013). Upregulated NLRP3 inflammasome activation in patients with type 2 diabetes. *Diabetes*, *62*(1), 194–204. https://doi.org/10.2337/db12-0420

Lieb, K., Fiebich, B. L., Busse-Grawitz, M., Hull, M., Berger, M., & Bauer, J. (1996). Effects of substance P and selected other neuropeptides on the synthesis of interleukin-1 beta and interleukin-6 in human monocytes: A re-examination. *Journal of Neuroimmunology*, *67*, 77–81. https://doi.org/10.1016/0165-5728(96)00034-3

Lilley, E., Stanford, S. C., Kendall, D. E., Alexander, S. P., Cirino, G., Docherty, J. R., George, C. H., Insel, P. A., Izzo, A. A., Ji, Y., Panettieri, R. A., Sobey, C. G., Stefanska, B., Stephens, G., Teixeira, M., & Ahluwalia, A. (2020). ARRIVE 2.0 and the British Journal of Pharmacology: Updated guidance for 2020. *British Journal of Pharmacology*, *177*(16), 3611–3616. https://bpspubs.onlinelibrary.wiley.com/doi/full/10.1111/bph.15178

Lin, H. H., Faunce, D. E., Stacey, M., Terajewicz, A., Nakamura, T., Zhang-Hoover, J., Kerley, M., Mucenski, M. L., Gordon, S., & Stein-Streilein, J. (2005). The macrophage F4/80 receptor is required for the induction of antigen-specific efferent regulatory T cells in peripheral tolerance. *The Journal of Experimental Medicine*, *201*(10), 1615–1625. https://doi.org/10.1084/jem.20042307

Lopez-Castejon, G., Luheshi, N. M., Compan, V., High, S., Whitehead, R. C., Flitsch, S., Kirov, A., Prudovsky, I., Swanton, E., & Brough, D. (2013). Deubiquitinases regulate the activity of caspase-1 and interleukin-1beta secretion via assembly of the inflammasome. *The Journal of Biological Chemistry*, *288*(4), 2721–2733. https://doi.org/10.1074/jbc.M112.422238

Luck, H., Tsai, S., Chung, J., Clemente-Casares, X., Ghazarian, M., Revelo, X. S., Lei, H., Luk, C. T., Shi, S. Y., Surendra, A., Copeland, J. K., Ahn, J., Prescott, D., Rasmussen, B. A., Chng, M. H. Y., Engleman, E. G., Girardin, S. E., Lam, T. K. T., Croitoru, K., … Winer, D. A. (2015). Regulation of obesity-related insulin resistance with gut anti-inflammatory agents. *Cell Metabolism*, *21*(4), 527–542. https://doi.org/10.1016/j.cmet.2015.03.001

Margolis, K. G., & Gershon, M. D. (2009). Neuropeptides and inflammatory bowel disease. *Current Opinion in Gastroenterology*, *25*, 503–511. https://doi.org/10.1097/MOG.0b013e328331b69e

Martin, F. C., Anton, P. A., Gornbein, J. A., Shanahan, F., & Merrill, J. E. (1993). Production of interleukin-1 by microglia in response to substance P: Role for a non-classical NK-1 receptor. *Journal of Neuroimmunology*, *42*, 53–60. https://doi.org/10.1016/0165-5728(93)90212-H

Martin, F. C., Charles, A. C., Sanderson, M. J., & Merrill, J. E. (1992). Substance P stimulates IL-1 production by astrocytes via intracellular calcium. *Brain Research*, *599*, 13–18. https://doi.org/10.1016/0006-8993(92)90846-2

Maslanik, T., Mahaffey, L., Tannura, K., Beninson, L., Greenwood, B. N., & Fleshner, M. (2013). The inflammasome and danger associated molecular patterns (DAMPs) are implicated in cytokine and chemokine responses following stressor exposure. *Brain, Behavior, and Immunity*, *28*, 54–62. https://doi.org/10.1016/j.bbi.2012.10.014

Masumoto, J., Taniguchi, S., Nakayama, J., Shiohara, M., Hidaka, E., Katsuyama, T., Murase, S., & Sagara, J. (2001). Expression of apoptosis-associated speck-like protein containing a caspase recruitment domain, a pyrin N-terminal homology domain-containing protein, in normal human tissues. *The Journal of Histochemistry and Cytochemistry: Official Journal of the Histochemistry Society*, *49*(10), 1269–1275. https://doi.org/10.1177/002215540104901009

Morimoto, A., Nakamori, T., Morimoto, K., Tan, N., & Murakami, N. (1993). The central role of corticotrophin-releasing factor (CRF-41) in psychological stress in rats. *The Journal of Physiology*, *460*, 221–229. https://doi.org/10.1113/jphysiol.1993.sp019468

Mushref, M. A., & Srinivasan, S. (2013). Effect of high fat-diet and obesity on gastrointestinal motility. *Annals of Translational Medicine*, *1*(2), 14.

Padilla, F., Couble, M. L., Coste, B., Maingret, F., Clerc, N., Crest, M., Ritter, A. M., Magloire, H., & Delmas, P. (2007). Expression and localization of the Nav1.9 sodium channel in enteric neurons and in trigeminal sensory endings: Implication for intestinal reflex function and orofacial pain. *Molecular and Cellular Neurosciences*, *35*, 138–152. https://doi.org/10.1016/j.mcn.2007.02.008

Palazon-Riquelme, P., Worboys, J. D., Green, J., Valera, A., Martin-Sanchez, F., Pellegrini, C., Brough, D., & López-Castejón, G. (2018). USP7 and USP47 deubiquitinases regulate NLRP3 inflammasome activation. *EMBO Reports*, *19*(10), e44766. https://doi.org/10.15252/embr.201744766

Pavillard, L. E., Canadas-Lozano, D., Alcocer-Gomez, E., Marin-Aguilar, F., Pereira, S., Robertson, A. A. B., Muntané, J., Ryffel, B., Cooper, M. A., Quiles, J. L., Bullón, P., Ruiz-Cabello, J., & Cordero, M. D. (2017). NLRP3-inflammasome inhibition prevents high fat and high sugar diets-induced heart damage through autophagy induction. *Oncotarget*, *8*, 99740–99756. https://doi.org/10.18632/oncotarget.20763

Pelegrin, P., & Surprenant, A. (2009). Dynamics of macrophage polarization reveal new mechanism to inhibit IL-1beta release through pyrophosphates. *The EMBO Journal*, *28*, 2114–2127. https://doi.org/10.1038/emboj.2009.163

Pellegrini, C., Antonioli, L., Lopez-Castejon, G., Blandizzi, C., & Fornai, M. (2017). Canonical and non-canonical activation of NLRP3 Inflammasome at the crossroad between immune tolerance and intestinal inflammation. *Frontiers in Immunology*, *25*(8), 36.

Pellegrini, C., Fornai, M., Colucci, R., Tirotta, E., Blandini, F., Levandis, G., Cerri, S., Segnani, C., Ippolito, C., Bernardini, N., Cseri, K., Blandizzi, C., Haskó, G., & Antonioli, L. (2016). Alteration of colonic excitatory tachykininergic motility and enteric inflammation following dopaminergic nigrostriatal neurodegeneration. *Journal of Neuroinflammation*, *13*(1), 146. https://doi.org/10.1186/s12974-016-0608-5

Percie du Sert, N., Hurst, V., Ahluwalia, A., Alam, S., Avey, M. T., Baker, M., Browne, W. J., Clark, A., Cuthill, I. C., Dirnagl, U., Emerson, M., Garner, P., Holgate, S. T., Howells, D. W., Karp, N. A., Lazic, S. E., Lidster, K., MacCallum, C. J., Macleod, M., … Würbel, H. (2020). The ARRIVE guidelines 2.0: Updated guidelines for reporting animal research. *PLoS Biology*, *18*(7), e3000410. https://doi.org/10.1371/journal.pbio.3000410

Pierantonelli, I., Rychlicki, C., Agostinelli, L., Giordano, D. M., Gaggini, M., Fraumene, C., Saponaro, C., Manghina, V., Sartini, L., Mingarelli, E., Pinto, C., Buzzigoli, E., Trozzi, L., Giordano, A., Marzioni, M., Minicis, S. D., Uzzau, S., Cinti, S., Gastaldelli, A., & Svegliati-Baroni, G. (2017). Lack of NLRP3-inflammasome leads to gut-liver axis derangement, gut dysbiosis and a worsened phenotype in a mouse model of NAFLD. *Scientific Reports*, *7*(1), 12200. https://doi.org/10.1038/s41598-017-11744-6

Rajindrajith, S., Devanarayana, N. M., & Benninga, M. A. (2014). Obesity and functional gastrointestinal diseases in children. *Journal of Neurogastroenterology and Motility*, *20*, 414–416. https://doi.org/10.5056/jnm14067

Raybould, H. E. (2012). Gut microbiota, epithelial function and derangements in obesity. *The Journal of Physiology*, *590*, 441–446. https://doi.org/10.1113/jphysiol.2011.222133

Reichardt, F., Baudry, C., Gruber, L., Mazzuoli, G., Moriez, R., Scherling, C., Kollmann, P., Daniel, H., Kisling, S., Haller, D., Neunlist, M., & Schemann, M. (2013). Properties of myenteric neurones and mucosal functions in the distal colon of diet-induced obese mice. *The Journal of Physiology*, *591*, 5125–5139. https://doi.org/10.1113/jphysiol.2013.262733

Rescigno, M. (2011). The intestinal epithelial barrier in the control of homeostasis and immunity. *Trends in Immunology*, *32*, 256–264. https://doi.org/10.1016/j.it.2011.04.003

Rheinheimer, J., de Souza, B. M., Cardoso, N. S., Bauer, A. C., & Crispim, D. (2017). Current role of the NLRP3 inflammasome on obesity and insulin resistance: A systematic review. *Metabolism, Clinical and Experimental*, *74*, 1–9. https://doi.org/10.1016/j.metabol.2017.06.002

Richter, S., D'Antongiovanni, V., Martinelli, S., Bechmann, N., Riverso, M., Poitz, D. M., Pacak, K., Eisenhofer, G., Mannelli, M., & Rapizzi, E. (2018). Primary fibroblast co-culture stimulates growth and metabolism in Sdhb-impaired mouse pheochromocytoma MTT cells. *Cell and Tissue Research*, *374*(3), 473–485. https://doi.org/10.1007/s00441-018-2907-x

Rodriguez-Hernandez, H., Simental-Mendia, L. E., Rodriguez-Ramirez, G., & Reyes-Romero, M. A. (2013). Obesity and inflammation: Epidemiology, risk factors, and markers of inflammation. *International Journal of Endocrinology*, *2013*, 678159.

Rugiero, F., Mistry, M., Sage, D., Black, J. A., Waxman, S. G., Crest, M., Clerc, N., Delmas, P., & Gola, M. (2003). Selective expression of a persistent tetrodotoxin-resistant Na+ current and NaV1.9 subunit in myenteric sensory neurons. *The Journal of Neuroscience: The Official Journal of the Society for Neuroscience*, *23*, 2715–2725. https://doi.org/10.1523/JNEUROSCI.23-07-02715.2003

Sage, D., Salin, P., Alcaraz, G., Castets, F., Giraud, P., Crest, M., Mazet, B., & Clerc, N. (2007). Na(v)1.7 and Na(v)1.3 are the only tetrodotoxin-sensitive sodium channels expressed by the adult guinea pig enteric nervous system. *The Journal of Comparative Neurology*, *504*(4), 363–378. https://doi.org/10.1002/cne.21450

Schmid-Burgk, J. L., Gaidt, M. M., Schmidt, T., Ebert, T. S., Bartok, E., & Hornung, V. (2015). Caspase-4 mediates non-canonical activation of the NLRP3 inflammasome in human myeloid cells. *European Journal of Immunology*, *45*, 2911–2917. https://doi.org/10.1002/eji.201545523

Shi, C. S., Shenderov, K., Huang, N. N., Kabat, J., Abu-Asab, M., Fitzgerald, K. A., Sher, A., & Kehrl, J. H. (2012). Activation of autophagy by inflammatory signals limits IL-1beta production by targeting ubiquitinated inflammasomes for destruction. *Nature Immunology*, *13*(3), 255–263. https://doi.org/10.1038/ni.2215

Souza, A. C. P., Souza, C. M., Amaral, C. L., Lemes, S. F., Santucci, L. F., Milanski, M., Torsoni, A. S., & Torsoni, M. A. (2019). Short-term High-fat diet consumption reduces hypothalamic expression of the nicotinic acetylcholine receptor alpha7 subunit (alpha7nAChR) and affects the anti-inflammatory response in a mouse model of sepsis. *Frontiers in Immunology*, *10*, 565. https://doi.org/10.3389/fimmu.2019.00565

Stenman, L. K., Holma, R., & Korpela, R. (2012). High-fat-induced intestinal permeability dysfunction associated with altered fecal bile acids. *World Journal of Gastroenterology*, *18*, 923–929. https://doi.org/10.3748/wjg.v18.i9.923

Steppan, C. M., Bailey, S. T., Bhat, S., Brown, E. J., Banerjee, R. R., Wright, C. M., Patel, H. R., Ahima, R. S., & Lazar, M. A. (2001). The hormone resistin links obesity to diabetes. *Nature*, *409*, 307–312. https://doi.org/10.1038/35053000

Stienstra, R., van Diepen, J. A., Tack, C. J., Zaki, M. H., van de Veerdonk, F. L., Perera, D., Neale, G. A., Hooiveld, G. J., Hijmans, A., Vroegrijk, I., van den Berg, S., Romijn, J., Rensen, P. C. N., Joosten, L. A. B., Netea, M. G., & Kanneganti, T. D. (2011). Inflammasome is a central player in the induction of obesity and insulin resistance. *Proceedings of the National Academy of Sciences of the United States of America*, *108*, 15324–15329. https://doi.org/10.1073/pnas.1100255108

Stoffels, B., Hupa, K. J., Snoek, S. A., van Bree, S., Stein, K., Schwandt, T., Vilz, T. O., Lysson, M., van't Veer, C., Kummer, M. P., Hornung, V., Kalff, J. C., de Jonge, W. J., & Wehner, S. (2014). Postoperative ileus involves interleukin-1 receptor signaling in enteric glia. *Gastroenterology*, *146*, 176–187, e171.

Strowig, T., Henao-Mejia, J., Elinav, E., & Flavell, R. (2012). Inflammasomes in health and disease. *Nature*, *481*, 278–286. https://doi.org/10.1038/nature10759

Tejera, D., Mercan, D., Sanchez-Caro, J. M., Hanan, M., Greenberg, D., Soreq, H., Latz, E., Golenbock, D., & Heneka, M. T. (2019). Systemic inflammation impairs microglial Abeta clearance through NLRP3 inflammasome. *The EMBO Journal*, *38*, e101064.

Troseid, M., Nestvold, T. K., Rudi, K., Thoresen, H., Nielsen, E. W., & Lappegard, K. T. (2013). Plasma lipopolysaccharide is closely associated with glycemic control and abdominal obesity: Evidence from bariatric surgery. *Diabetes Care*, *36*, 3627–3632. https://doi.org/10.2337/dc13-0451

Vallejo, S., Palacios, E., Romacho, T., Villalobos, L., Peiro, C., & Sanchez-Ferrer, C. F. (2014). The interleukin-1 receptor antagonist anakinra improves endothelial dysfunction in streptozotocin-induced diabetic rats. *Cardiovascular Diabetology*, *13*(1), 158. https://doi.org/10.1186/s12933-014-0158-z

Vandanmagsar, B., Youm, Y. H., Ravussin, A., Galgani, J. E., Stadler, K., Mynatt, R. L., Ravussin, E., Stephens, J. M., & Dixit, V. D. (2011). The NLRP3 inflammasome instigates obesity-induced inflammation and insulin resistance. *Nature Medicine*, *17*(2), 179–188. https://doi.org/10.1038/nm.2279

Yang, G., Lee, H. E., & Lee, J. Y. (2016). A pharmacological inhibitor of NLRP3 inflammasome prevents non-alcoholic fatty liver disease in a mouse model induced by high fat diet. *Scientific Reports*, *6*, 24399. https://doi.org/10.1038/srep24399

Yang, S. J., & Lim, Y. (2014). Resveratrol ameliorates hepatic metaflammation and inhibits NLRP3 inflammasome activation. *Metabolism, Clinical and Experimental*, *63*, 693–701. https://doi.org/10.1016/j.metabol.2014.02.003

SUPPORTING INFORMATION

Additional supporting information may be found online in the Supporting Information section at the end of this article.

How to cite this article: Pellegrini, C., Fornai, M., Benvenuti, L., Colucci, R., Caputi, V., Palazon-Riquelme, P., Giron, M. C., Nericcio, A., Garelli, F., D'Antongiovanni, V., Segnani, C., Ippolito, C., Nannipieri, M., Lopez-Castejon, G., Pelegrin, P., Haskó, G., Bernardini, N., Blandizzi, C., & Antonioli, L. (2021). NLRP3 at the crossroads between immune/inflammatory responses and enteric neuroplastic remodelling in a mouse model of diet-induced obesity. *British Journal of Pharmacology*, 1–19. https://doi.org/10.1111/bph.15532